



Review

Photocatalysts for chemical-free PFOA degradation – What we know and where we go from here?

Jan-Max Arana Juve^{a,b}, Juan A. Donoso Reece^b, Michael S. Wong^b, Zongsu Wei^{a,*}, Mohamed Ateia^{b,c,**}

^a Centre for Water Technology (WATEC) & Department of Biological and Chemical Engineering, Aarhus University, Universitetsbyen 36, 8000 Aarhus C, Denmark

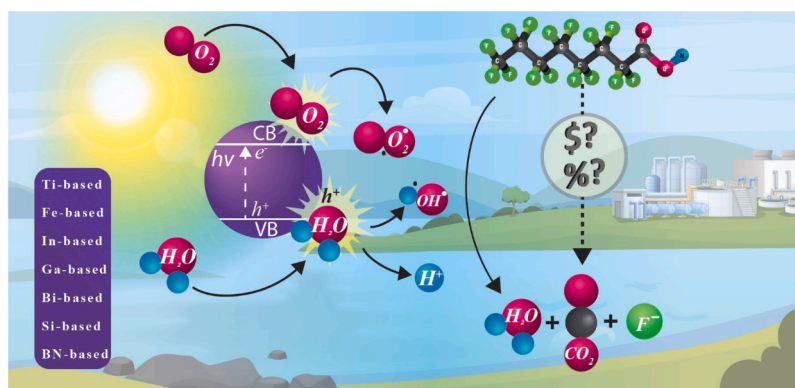
^b Department of Chemical and Biomolecular Engineering, Rice University, Houston, TX, USA

^c Center for Environmental Solutions & Emergency Response, US Environmental Protection Agency, Cincinnati, OH, USA

HIGHLIGHTS

- State-of-the-art of chemical-free photocatalysts families for PFOA degradation.
- Evaluation of the performance and practical limitations of the photocatalysts.
- Discussion of the strategies to enhance the material's performance.
- A cost evaluation tool estimates the material cost and compares the performance.
- Identification of current research gaps and future research opportunities.

GRAPHICAL ABSTRACT



ARTICLE INFO

Editor: Lingxin Chen

Keywords:

PFOA defluorination
Photocatalysis
Chemical-free
Cost evaluation
Catalyst design

ABSTRACT

Perfluorooctanoic acid (PFOA) is a toxic and recalcitrant perfluoroalkyl substance commonly detected in the environment. Its low concentration challenges the development of effective degradation techniques, which demands intensive chemical and energy consumption. The recent stringent health advisories and the upgrowth and advances in photocatalytic technologies claim the need to evaluate and compare the state-of-the-art. Among these systems, chemical-free photocatalysis emerges as a cost-effective and sustainable solution for PFOA degradation and potentially other perfluorinated carboxylic acids. This review (I) classifies the state-of-the-art of chemical-free photocatalysts for PFOA degradation in families of materials (Ti, Fe, In, Ga, Bi, Si, and BN), (II) describes the evolution of catalysts, identifies and discusses the strategies to enhance their performance, (III) proposes a simplified cost evaluation tool for simple techno-economical analysis of the materials; (IV) compares the features of the catalysts expanding the classic degradation focus to other essential parameters, and (V) identifies current research gaps and future research opportunities to enhance the photocatalyst performance. We

* Corresponding author.

** Corresponding author at: Department of Chemical and Biomolecular Engineering, Rice University, Houston, TX, USA.

E-mail addresses: zwei@bce.au.dk (Z. Wei), ibrahim.mohamed@epa.gov (M. Ateia).

<https://doi.org/10.1016/j.jhazmat.2023.132651>

Received 25 June 2023; Received in revised form 11 August 2023; Accepted 26 September 2023

Available online 29 September 2023

0304-3894/Published by Elsevier B.V.

aim that this critical review will assist researchers and practitioners to develop rational photocatalyst designs and identify research gaps for green and effective PFAS degradation.

1. Introduction

Per- and polyfluoroalkyl substances (PFAS) are widely distributed persistent pollutants that pose various adverse effects on human health, e.g., carcinogenicity, cell membrane disruption, neurotoxicity, endocrine disruptor, and among others [1,2]. Perfluorooctanoic acid (PFOA) is the most iconic PFAS compound [3] released into the water systems from direct industrial discharge, air emissions, landfill leachate, and firefighter foams. The structure of PFOA is highly stable because the hydrogen atoms of the hydrocarbon chain are fully substituted with fluorine atoms, and the C–F bond (536 kJ/mol) [4] confers high stability to the molecule favoring its introduction and bioaccumulation in living organisms [5]. Furthermore, PFOA is typically found in $\mu\text{g/L}$ to ng/L concentrations, which challenges the application of conventional separation and degradation technologies. The primary and secondary treatments in wastewater treatment plants (WWTPs) are not effective to remove and degrade PFAS [6,7], making WWTPs point sources for these contaminants discharged into the aquatic environment [8]. The addition of tertiary treatments becomes a must even though the treatment costs increase [9]. Therefore, chemical-free and low energy-demanding treatments are preferred to deal with high water volumes, since they do not involve chemical consumption which decreases the process costs and environmental friendliness of the processes. Besides, the ever-stringent proposed regulation limit of 4 ng/L for PFOA in the US [10] and 0.5 $\mu\text{g/L}$ for all PFAS in the EU [11] along with the new upcoming regulations [12] attract intensive interest to find economically feasible solutions for PFAS removal and degradation (Fig. 1).

In recent years, photocatalysis has emerged as one of the main research technologies in water treatments (Fig. 1) [13], due to its high defluorination efficiency on PFOA, mild pH and temperature conditions, low energy consumption, sustainability of the process [14], synergistic capacity with other treatment methods (e.g., concentration technologies). However, photocatalysis-based technologies require further efforts to overcome critical drawbacks such as restricted light absorption

range, low quantum yield, lack of stable/reusable materials, or dependence on the water matrices. Meanwhile, it was found degradation of perfluoroalkyl carboxylic acids (PFCAs) is easier over perfluoroalkyl sulfonic acids since the last require 3 times higher C–F bond activating energy compared to PFCAs [15]. Thus, photocatalysis is a preferred technology for PFOA degradation, which results in short-chain byproducts, fluoride ions (F^-), and innocuous species (e.g., CO_2 , H_2O). In this review, we use the term degradation for the PFOA fraction transformed to byproducts and the term defluorination for the F^- fraction produced due to PFOA destruction. It is worth noting that only a few studies focus on the defluorination efficiency (Fig. 1, inset), which is critical to eliminate the associated toxicity related to short-chain byproducts[2]. The length and charged nature of short-chain PFAS increase the mobility [16] and solubility [17] of these compounds opening new paths to bioaccumulate and interact with biological processes and molecules [18].

As we will expand on in later sections, PFOA photodegradation varied depending on parameters such as irradiation wavelength, catalyst dose, and concentration. Thus, the development of novel photocatalysts and understanding the effect of operating parameters are key to promoting PFOA degradation. Despite the recent upgrowth in the number of published works, it remains challenging to directly compare photocatalysts operated under different parameters. The difficulty scales up when comparing different PFCAs. Given the urgency to find suitable PFAS solutions and the upswing of photocatalysis as a sustainable green technology, it is necessary and timely to evaluate and rationalize the current state-of-the-art of photocatalysis. To this end, we use PFOA in this work as a model long-chain PFCA due to the significant data availability with photocatalytic technologies compared to other PFAS. This critical review starts by introducing the main families of materials for PFOA photocatalytic degradation to compare their performance, practical strengths, and drawbacks. Then, we discuss the main strategies for effective photocatalytic degradation of PFOA and provide insights on future research trends to overcome the limitations of traditional

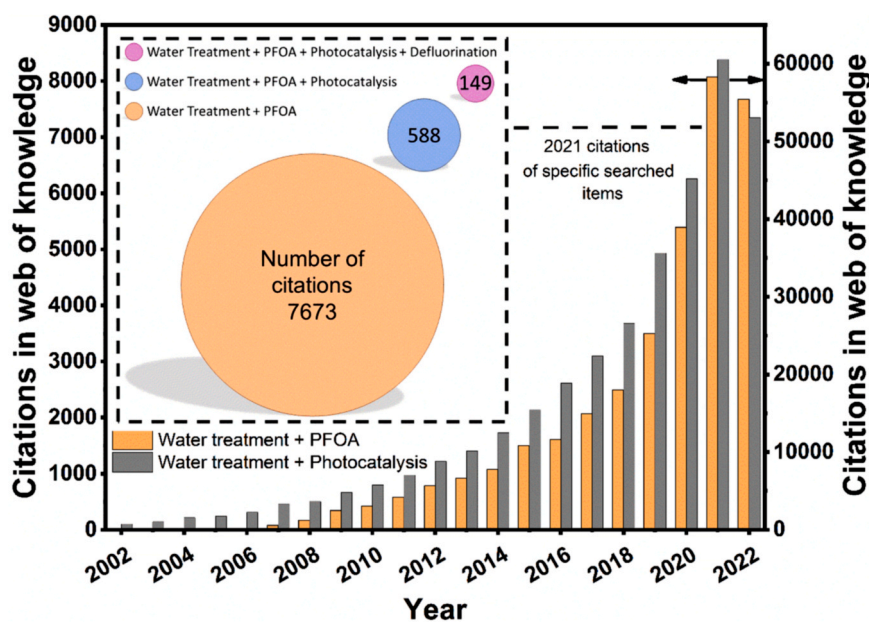


Fig. 1. Overview of the published literature on water treatment using photocatalysts and the interest in PFAS in water treatment over the past 20 years. Results from the web of knowledge (populated on Dec. 7th, 2022) for the period from 2002 to 2022. The inset shows the results of 2021 for “Water Treatment”, and “PFOA” with an inclusion relationship of the terms “Photocatalysis” and “Defluorination”.

photocatalysts.

2. Chemical-free photocatalysts for PFOA degradation

This section structures, discusses, and compares the main families of photocatalysts (Ti, Fe, Ga, In, Bi, Si, and BN) and their performance. A previous literature study [19] classified the photodecomposition performance of PFAS photocatalysts families as $\text{In}_2\text{O}_3 > \text{Ga}_2\text{O}_3 > \text{TiO}_2$, while newer reports include Bi-materials [20]. However, current literature does not include novel materials, which tend to overcome the practical limitations of classic photocatalysts. Literature summaries also omit the difference between chemical and chemical-free systems and they are unspecific for different PFAS, which challenges the effective comparison between works (Table S1).

In this section, we aim to determine the effectiveness and evolution of the photocatalyst families, through the generation of reactive species (RS), understanding the differences in the photocatalytic degradation mechanisms. The RS are produced with a light source emitting irradiation with a certain wavelength, that determines the photon energy, to excite the electrons of semiconductors. Most literature studies were performed under Ultraviolet (UV) light C (100–280 nm), typically 254 nm. Although PFOA photodegradation was also reported under UVB (280–320 nm), UVA (320–400 nm), and even sunlight. Photochemically generated RS including hydroxyl radicals ($\bullet\text{OH}$), superoxide ($\bullet\text{O}_2^-$), singlet oxygen ($^1\text{O}_2$), and holes (h^+) are hypothesized as PFOA degradation pathway initiators.

Photocatalysts typically degrade PFOA through h^+ -mediated oxidation [21–23] at the valence band (VB) following a stepwise defluorination mechanism. The h^+ degradation depends on I) the interaction capacity between the h^+ and the PFOA molecule; II) the sufficient oxidative potential for the photogenerated h^+ to degrade PFOA (Table S2); and III) the abundance and availability of h^+ to complete the PFOA degradation. From a thermodynamic perspective, the h^+ -oxidation is favored when the maximum VB potential is more positive than the potential needed to form a perfluorocarboxyl radical [24] (2.18 eV vs Normal Hydrogen Electrode (NHE) [25]). Avoiding electron-hole recombination, and maximizing the RS production can also enhance the kinetics of the process [26]. The roles of other photocatalytic RS on the PFOA degradation mechanisms are still under debate (Fig. 2A). For example, the $\bullet\text{OH}$ (2.31 eV vs NHE [27]) is ineffective for most PFOA degradation processes since it cannot break the C–F bond [28]. Therefore, novel pathways are needed to justify the facilitating role of $\bullet\text{OH}$, if any, in the degradation mechanisms [25,26]. Similarly, $\bullet\text{O}_2^-$ degradation (0.91 eV vs NHE [27]) has been reported as the main RS for PFOA [29,30], but recent reports claim $\bullet\text{O}_2^-$ might not be initiating the degradation process [21]. However, $\bullet\text{O}_2^-$ may still be relevant in some cases, such as activated systems decarboxylation [21] and facilitating the degradation of byproducts [26]. $^1\text{O}_2$ (0.81 eV vs NHE

[27]) is a widely known RS in chemical-free systems, however, it is scarcely discussed in PFOA-degrading systems. Initial PFOA decarboxylation and byproduct degradation with $^1\text{O}_2$ was proposed after major degradation inhibition with L-histidine[31]; however, additional scavenging tests with 2,2,6,6-tetramethylpiperidine report that $^1\text{O}_2$ can not initiate the decarboxylation [32]. Finally, photogenerated hydrated electrons (e_{aq}^-) are effective PFOA-degrading species through advanced reduction processes (ARPs) [33–35]. Noble metals like Pt are commonly employed to promote electron trapping and C–F bond activation for direct F^- extraction or intermediate radical formation [34,36,37]. However, electron attacks preferentially occur in anoxic conditions due to the fast scavenging capacity of oxygen ($k = 1.9 \times 10^{10} \text{ M}^{-1} \text{ s}^{-1}$) [38]. Interestingly, the recent interest in systems based on vacuum UV (VUV) with wavelengths shorter than 200 nm showed direct PFOA degradation in catalyst-free and chemical-free processes. PFOA was decarboxylated by forming unstable perfluoroalkyl radicals that are further decomposed to shorter-chain PFAS [39–41]. It is worth noting that monitoring VUV and its contribution in PFOA degradation is fundamentally critical to differentiate the influence of catalysts, simple irradiation, and synergistic effects.

2.1. Titanium-based photocatalysts

TiO_2 and its derivatives are attractive for PFOA degradation due to their abundance, low cost, and broad acceptability. TiO_2 typically presents limited defluorination efficiency (<10%) [36,43–46] compared to other PFOA degrading materials. However, high PFOA concentrations below critical micelle concentration (i.e., $<7.80 \times 10^{-3} \text{ mol L}^{-1}$ at 25 °C) can be defluorinated between 22% [47] and 29% [48] after up to 6 h treatments. These studies demonstrated surface modification due to F^- ions incorporation in the TiO_2 crystalline structure, which may warrant further studies to verify the role of crystallinity in controlling defluorination. However, surface modification may present a drawback in terms of catalyst stability and leaching. Likewise, TiO_2 derivatives such as titanate nanotubes (TNTs) are positively charged at pH 4 [49], which promotes electrostatic interactions. Besides, TNTs typically present a higher specific surface area, resulting in more active sites for the PFOA molecules. However, modest PFOA defluorination is observed (i.e. <10% in 8 h) [49,50]. Overall, the low performance of Ti-based materials drove research attention to two main strategies: I) adding doping agents, and II) preparing composites coupled with carbonaceous materials to enhance the adsorption and promote the interaction between the photogenerated RS and PFAS degradation (Table 1).

2.2. Doping of TiO_2

The addition of a doping agent can modify the structure, the optical properties of the materials and form heterojunctions with the

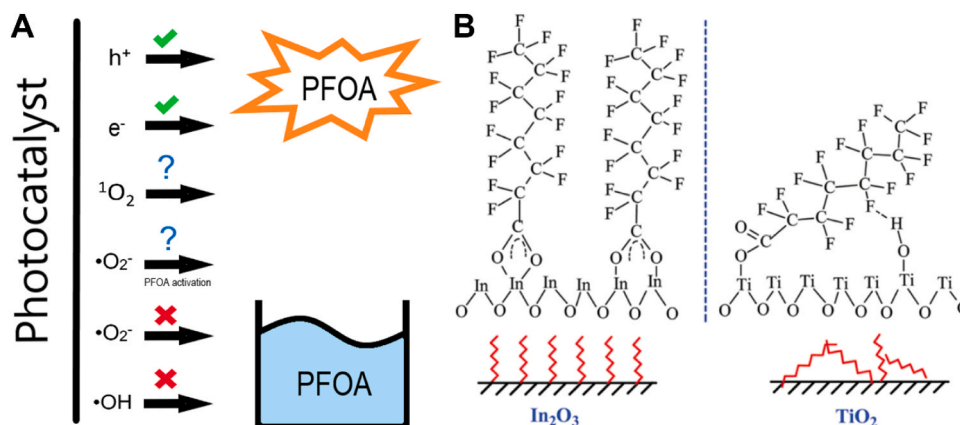


Fig. 2. A) PFOA degradation by photogenerated RS; B) Bidentate (In_2O_3) and monodentate (TiO_2) adsorption mechanisms[42].

Table 1

Summary of parameters for metal-doped Titanium-based composites for PFOA defluorination (Simulated sunlight = SS; *check the work for details).

Catalyst	Dose, g L ⁻¹	Pollutant, mg L ⁻¹	Power, W	pH	Time, h	Wavelength, nm	Removal, %	Defluorination %	Ref
TiO ₂	0.66	1656	500	-	6	310–400	~30	22	[47]
TiO ₂	0.66	1656	500	-	6	315–400	~44	29	[48]
TNT	0.2	30	23	5	8	254	> 40	5.4	[50]
TNT	0.25	50	400	4	24	254	59	< 5	[49]
TiO ₂	0.5	50	400	5	12	254	14	-	[43]
TiO ₂	0.5	50	400	5	12	254	18.3	-	[44]
TiO ₂	0.5	60	125	3	7	365	31.1	3.3	[46]
Fe-TiO ₂	0.5	50	400	5	12	254	69	9	[43]
Cu-TiO ₂	0.5	50	400	5	12	254	91	19	[43]
Pb-TiO ₂	0.5	50	400	5	12	254	> 99	22.4	[44]
Ag-TiO ₂	0.5	60	125	3	7	365	57.7	8.1	[46]
Fe:Nb-TiO ₂	0.5	41,4	150	4.3	3	200–600	~14	-	[45]
Pd-TiO ₂	0.5	60	125	3	7	365	94.2	25.9	[46]
Pt-TiO ₂	0.5	60	125	3	7	365	> 99	34.8	[46]
SA Pt-TiO ₂	0.25	41,4	5	-	2	254	< 40	~40	[36]
Sb ₂ O ₃ -TiO ₂	0.25	1	4	3.5	2	254	~82	-	[51]
Ce-Co-TiO ₂	0.50	1	450	6	1.5	200–410	> 99	74.8	[53]
F-MOF-TiO ₂	0.02	124.2	400	-	10	SS	> 90	~37.5	[66]
TiO ₂ -MWCNT	1.6	30	300	5	8	365	94	-	[55]
TiO ₂ -GO	*	0.05	8	7	3	254	~50	1.5	[61]
TiO ₂ -rGO	0.1	~100	150	3.8	12	200–600	93	20	[142]
TiO ₂ -GO	0.2	~5	8	4–5	8	254	93.6	-	[62]
TiO ₂ -rGO	0.2	~5	8	4–5	8	254	99.2	-	[62]
TiO ₂ -rGO	0.1	~100	150	3.8	8	200–600	~80	~30	[131]
TiO ₂ -PTFE	0.4	50	18	4	5	254	~80	< 40	[67]
TiO ₂ -GO	0.4	50	18	4	5	254	> 80	~40	[67]
TiO ₂ -PE	0.4	50	18	4	5	254	~90	~50	[67]
SG-TiO ₂ -QD	20	~125	150	7	10	200–600	> 90	35	[64]
IP-TNT	-	30	23	5	8	254	84	30.2	[50]
In/TNT@AC	1	0.1	18	7	4	254	> 99	~60	[57]
Fe/TNT@AC	1	0.1	18	7	4	254	> 99	62	[56]

semiconductor materials. This strategy enhances the PFOA defluorination by promoting electron trapping, decreasing the bandgap, and/or shifting the zero-point charge (PZC) of the composite in favor of PFOA-catalyst interaction. The structural distortion of the doped metals in the semiconductor lattice can create oxygen vacancies (OVs) [45], which affects the UV/Vis absorption of the material and therefore the bandgap properties and the energy required to excite the electron. For example, TiO₂ modified with Fe and Cu resulted in defluorination values of 9% and 19%, respectively [43], since the higher conductivity of Cu favors electron trapping and thus PFOA defluorination. Other composites such as Pb-TiO₂ (~99.9% degradation and >22% defluorination) [44] and Sb₂O₃-TiO₂ (double degradation rate vs commercial TiO₂) [51] also favored the breakdown of PFOA molecules. Similarly, codoped TiO₂ with Nb and Fe also improved the degradation of PFOA by ~15% compared to commercial TiO₂ [45]. However, the use of toxic metals should be limited to the strictly necessary application since it challenges the green chemistry principles. Additionally, the leaching of those toxic metals should be carefully monitored to avoid additional treatment technologies [52].

The high conductivity of precious metals Ag, Pd, and Pt increased the defluorination of PFOA to 8.1%, 25.9%, and 34.8%, respectively after 7 h of irradiation [46]. Specifically, Pt-TiO₂ degraded 50% PFOA anions in just 2 h, due to the electron trapping capacity and positive charge of Pt [46]. Further investigations lead to a method to site-selectively load single-atom Pt onto TiO₂, which formed a semiconductor-metal (S-M) heterojunction with an increased number of active sites per unit mass of Pt. The new composite achieved ~40% defluorination of PFOA in 2 h [36]. The reductive mechanism consists of C–F bond activation, and hydrodefluorination onto the Ti-surface. While evaluating these catalysts, it is necessary to extract and characterize the analytes on the surface of the material after degradation to obtain reliable mass balances. Recently, complex materials such as a trimetallic-oxide, based on Ti, Ce, and Co, with PZC at 8.5, defluorinated 74.8% of PFOA within 90 min [53]. Note that Ce is one of the most electropositive elements, which can favor the electrostatic interaction with the PFOA anions.

Therefore, doping materials with electropositive atoms such as Ca, Mg, or Ce (Table S3) may improve the adsorption and degradation, not only for PFOA but also for other anionic PFAS and micropollutants.

2.2.1. Carbonaceous titanium-based composite materials

Ti materials have been coupled with carbonaceous materials for micropollutants remediation [54], due to their high surface area and relatively low cost. For example, adsorptive multi-walled carbon nanotubes (MWCNT) coupled with TiO₂ demonstrated an increase in the adsorption of PFOA by 7% compared to TiO₂. However, the PFOA removal after 8 h increased by 41% [55]. Recently, a composite coupling TNT with activated carbon (AC) adsorbed as much as 80.2 mg PFOA g⁻¹, although the defluorination remained modest (<20% in 4 h) [56]. Hence, doping of TNT@AC-based materials with Fe, In, and Ga [56–60] was tested to form a multicomponent heterojunction reaching ~50% defluorination in 4 h.

Graphene oxide (GO) and reduced GO (rGO) are among the most popular carbon materials due to their high surface area, 2D structure, and excellent electrical conductivity. TNT@GO composite material could effectively degrade 30% of PFOA in 3 h, although the defluorination rate was just 1.5% [61]. In comparison, TiO₂@GO and TiO₂@rGO composites obtained 93.6% and 99.2% degradation of PFOA in 8 h, respectively [62]. The rGO presents fewer functional groups, which increases its conductivity and electron trapping capacity. Furthermore, the enhanced defluorination performance of TiO₂@rGO suggests that the hydrophobic structure enhances the electron trapping capacity of rGO. Despite the effective semiconductor-carbon (S-C) heterojunction with TiO₂, GO and rGO materials play a limited role in the adsorption of PFOA. The low PFOA adsorption of GO/rGO can be attributed to its negative surface charge under neutral pH [63], given the PZC of ~2.8 for rGO and negative charge for GO along the pH range (2–12). Functionalized graphene materials, such as sulfonated graphene aerogel (SGA) loaded onto TiO₂ quantum dots (SGA-TiO₂-QD) could adsorb 0.17–0.19 mmol PFOA g⁻¹ [61] and defluorinated up to ~35% of the adsorbed PFOA in 10 h [64]. Amination also promotes adsorption

achieving a positive surface charge at neutral pH [65]. Besides carbonaceous adsorbents, novel adsorptive photocatalysts were designed to concentrate and destroy PFOA. This includes molecularly-imprinted acrylamide polymers coupled with TNT [50] and TiO₂ coupled with metal-organic-frameworks (MOFs) [66]. A novel study proposed a novel role of the TiO₂ carbon-based heterojunctions comparing GO and non-conductive polymers such as (e.g., polyethylene, polytetrafluoroethylene). The results also suggest that the potential charge separation of GO did not significantly contribute to PFOA degradation, but the formed heterojunction was responsible for a dual PFOA adsorption mechanism based on hydrophobic and electrostatic interactions that promoted its degradation [67].

2.3. Iron-based photocatalysts

Iron-based catalysts present high defluorination efficiencies besides their magnetic properties and low costs. Zn, Cu, Mg, and Mn ions show very limited defluorination of PFOA [68], compared to Fe³⁺. The superior photodegradation properties suggest unique Fe³⁺ complexation properties for PFOA (Table 2), which are different from other metal oxides and cations. Fe complexation decreases the decarboxylation energy of PFOA from 396.19 kJ/mol in the anion form to 370.41 kJ/mol in the complexed system [69], which is not reported for other cations. The mechanism is based on a ligand-to-metal charge transfer (LMCT) upon light irradiation [40,41,68], which opens a research line to understanding ion-PFAS interactions. Initial research on PFOA degradation using Fe species focused on Fe³⁺ ions irradiation (i.e., not using solid catalysts) and the mechanism did not follow classic photodegradation pathways. In Fe³⁺/VUV systems Fe³⁺ complexate PFOA, which favors its decarboxylation. The process results in a two-fold increase in the defluorination rate compared to VUV systems [41]. Besides catalyst dose [68], the irradiation source is also critical: VUV systems [41] present a 51.21% defluorination, while UVC [68] present 31.2% in 4 h with similar Fe³⁺ doses (30–40 μM). In fact, complete defluorination was achieved after 72 h using VUV and Fe³⁺[40], demonstrating the potential and effectiveness of Fe ions for PFOA treatment. In this context, sunlight decomposition of the Fe³⁺/PFOA system can achieve complete removal of PFOA under 28 days of irradiation, yet low defluorination (12.7%) [70]. The pH is a critical parameter in Fe-systems since it determines the Fe phases, the reaction mechanisms, and the defluorination performances [71].

The Fe-based solid catalysts did not outperform Fe-ions systems. Apparently, the difference in the defluorination efficiency is due to the less effective PFOA complexation. For example, zero-valent iron (ZVI) nanoparticles (NPs) only exhibited a moderate degradation rate (~15% in 25 h) [72]. Interestingly, Qian et al. [73] designed a novel composite using a hydrophobic zeolite adsorbent with low Fe content (1.3%). Interestingly, this material presented high PFOA defluorination (~40% in 24 h) under UVA light at a relatively high pH of 5.5 by combining the homogeneous catalytic properties of Fe ions and the heterogeneous catalysis nature of zeolites. Similarly, concentrate-and-destroy catalysts combining carbonaceous and Fe-based materials have also been developed to facilitate catalyst recovery and overcome pH limitations for Fe ions-based catalysts [74].

Table 2

Summary of parameters for Iron-based composites for PFOA defluorination (* equals μM).

Catalyst	Dose, g L ⁻¹	Pollutant, mg L ⁻¹	Power, W	pH	Time, h	Wavelength, nm	Removal, %	Defluorination %	Ref
Fe ³⁺	80 *	20	23	< 4	4	254	80.2	47.8	[68]
Fe ³⁺	480 *	~20	24	4.6	672	SS	97.8	12.7	[70]
Fe ³⁺	12 *	~15	12	< 4	4	185 & 254	> 85	51.2	[41]
Fe ³⁺	20 *	~15	5	< 4	72	185 & 254	> 99	> 99	[40]
Fe ³⁺	50 *	~20	14	2	4	254	> 99	> 99	[71]
Fe(0)	0.1	1	112	4.8	25	254	58	> 15	[72]
Fe-BEA	0.5	20	4	5.5	24	365	> 99	38	[73]
FeO/CS	1	0.2	18	7	4	SS	95.2	57.2	[74]

2.4. Post-transition metal-based photocatalysts

Post-transition metal catalysts can complex and activate the PFOA molecules at the catalyst surface (Fig. 2B) [42]. The most studied post-transition metals of Ga, In, and Bi are rare and expensive, therefore it is critical to optimize the material design by increasing the catalyst recovery, ensuring the catalyst reusability, and minimizing the dose and the leaching.

2.4.1. Gallium catalysts

Gallium oxide exists in 5 different phases, among which β-Ga₂O₃ is the only stable phase [75]. The bandgap (4.18 eV) of β-Ga₂O₃ requires energetic wavelengths (<300 nm) for effective charge separation. Table 3 summarizes the parameters for the discussed gallium-based composites for PFOA degradation. The PFOA degradation mechanism by β-Ga₂O₃ is still inconclusive. Under N₂ atmosphere, 40% degradation and 15% defluorination of PFOA in 3 h were observed [76]. The presence of N₂ is essential since O₂ scavenges the e_{aq}⁻ inhibiting the reaction [76,77], likely due to the production of hydrogen peroxide [76]. The high conduction band (CB) potential (-2.95 eV vs vacuum) for β-Ga₂O₃ permits a direct reaction between PFOA and e_{aq}⁻[77]. However, other studies suggested that h⁺ played a major role in PFOA degradation [78], which was confirmed by quenching •OH and h⁺ using tert-butanol and ammonium oxalate, respectively [79].

Nanocomposite facet engineering and design is a useful tool to promote photodegradation. Among the developed nanostructures, needle-like β-Ga₂O₃ doubled the surface area and degraded PFOA 7.5 times faster than commercial β-Ga₂O₃, reaching 58% defluorination in 3 h [78]. Sheaf-like β-Ga₂O₃ also enhanced the surface area and promoted a preferentially exposed (100) crystal facet, compared to TiO₂ (001). This bidentated PFOA and completely degraded PFOA in 45 min, which is much higher than commercial β-Ga₂O₃ (~25% in 45 min) [80]. β-Ga₂O₃ nanorods (NRs) achieved similar results under anoxic conditions (98.8% degradation and 56.2% defluorination) in just 90 min [81]. Ga₂O₃ nanosheets (NSTs) were modified with different metals (M = In, Cu, Zn, Co, and Mn). Among them, In-Ga₂O₃ NSTs composite created a straddling gap heterojunction which degraded PFOA 7.8 times faster than pristine Ga₂O₃, increasing the defluorination in 4 h from 13% to 57% at pH 4.5 [79]. The high performance of Ga materials encourages its further use for PFOA degradation; however, the scarcity and high price limit its practical application, resulting in its limited use as a doping agent.

2.4.2. Indium-based photocatalysts

A direct comparison of the PFOA degradation with TiO₂ demonstrated the superior capacity of In₂O₃[42]. The positive charge, bidentate adsorption mechanism (Fig. 2B), and the optical properties of indium enhanced the degradation by ~65%, compared to TiO₂, reaching defluorination values over 30% in 4 h [42]. Similarly, InOOH could improve by 27 times the PFOA degradation compared to commercial P25 [82]. The relatively small bandgap of In₂O₃ (~2.8 eV) reduces the energy required to excite an electron. However, the computationally calculated redox potential to form a perfluorocarboxyl radical (2.18 eV vs NHE) [25] is close to the maximum reported VB of In₂O₃

Table 3
Summary of parameters for Gallium-based composites for PFOA defluorination.

Catalyst	Dose, g L ⁻¹	Pollutant, mg L ⁻¹	Power, W	pH	Time, h	Wavelength, nm	Removal, %	Defluorination %	Ref
β-Ga ₂ O ₃	0.5	40	15	-	3	254	~40	~15	[77]
β-Ga ₂ O ₃	0.5	~31	15	-	3	254	43.6	~15.7	[76]
Needle-like β-Ga ₂ O ₃	0.5	0.5	14	4.8	3	254	> 99	58	[78]
sheaf-like β-Ga ₂ O ₃	0.5	~0.5	14	~4.7	3	254	> 99	> 60	[80]
sheaf-like β-Ga ₂ O ₃	1.8	~54	18	~4	2	254	> 60	~30	[116]
NRs β-Ga ₂ O ₃	0.5	10	50	3.8	1.5	254	98.8	56.2	[81]
In-Ga ₂ O ₃ NSTs	0.5	20	200	4.5	4	200–1000	> 99	57	[79]
In ₂ O ₃	0.5	41.4	23	3.8	4	254	80	~30	[42]
In ₂ O ₃ NPs	0.5	30	23	3.9	3	254	> 90	29.7	[83]
In ₂ O ₃ NCs	0.5	30	15	3.9	2	254	> 99	-	[84]
In ₂ O ₃ NPTs	0.5	30	15	4.2	1.5	254	53.50	21.33	[22]
In ₂ O ₃ NPTs	0.5	30	15	3.9	0.67	254	> 99	-	[84]
In ₂ O ₃ porous NPTs	0.5	30	15	-	0.5	254	> 99	-	[85]
In ₂ O ₃ Microspheres	0.5	30	15	3.9	0.33	254	> 99	-	[84]
InOOH	0.25	20	18	-	3	254	83.4	~18	[82]
In heterojunctions	0.33	20	100	-	7	254	85.5	-	[87]
In ₂ O ₃ NSTs hetero	0.4	200	500	-	1	-	96	-	[86]
In ₂ O ₃ NSPs	0.5	30	23	3.9	3	254	> 99	71.0	[83]
In ₂ O ₃ NSPs	0.2	10	32	-	8	254	> 99	~56	[88]
In ₂ O ₃ NRs	0.2	10	32	-	8	254	> 99	~48	[88]
N-doped In ₂ O ₃	0.125	0.414	350	5	6	> 250	~90	36.1	[89]
In ₂ O ₃ -Graphene	0.5	30	15	-	3	254	> 99	60.9	[91]
CeO ₂ -In ₂ O ₃	0.4	100	500	2.84	1	UV	> 99	53.3	[93]
Pt-In ₂ O ₃ NRs	0.4	200	500	1.85	1	UV	98	-	[94]
MnO _x -In ₂ O ₃	0.5	50	500	3.8	3	UV	99.8	17.4	[92]
Fe ³⁺ -In ₂ O ₃	0.5	10	32	~4	4	254	> 99	~30	[90]

nanostructures (2.17–2.44 eV vs NHE, Table S2). This situation points out the importance of the valence band characterization to demonstrate the thermodynamically favored PFOA h^+ -oxidation. Unlike gallium, research on indium materials includes the development of nanostructures and the development of composite materials (Table 3).

2.4.2.1. Indium nanostructures. The modification of surface and structural properties was also adopted for In₂O₃ nanocrystals and nanospheres (NSPs). The NSPs presented uniform size and higher surface area (39.0 m² g⁻¹) compared to commercial In₂O₃ nanocrystals (12.7 m² g⁻¹). Compared to commercial TiO₂, the NSPs, and nanocrystals enhanced the PFOA adsorption by over 25% and 15%, respectively, and the defluorination rates were above 20% for nanocrystals and 65% for NSPs [83]. Other morphologies such as nanocubes (NCs), nanoplates (NPTs), and porous microspheres increased the surface area, to 13.6, 18.9, and 42.3 m² g⁻¹, respectively. As expected, the microspheres outperformed NCs and NPTs materials, with complete PFOA degradation in 20 min. According to XPS tests, the microspheres presented a higher density of defects named OV, compared to NPTs and NCs, which promoted bidentate adsorption of PFOA [84]. Micro-sized materials are attractive options in water treatment applications because of their practical recovery.

In the synthesis process, control of the process parameters is critical to tune the crystalline structure of catalysts. For example, ethylenediamine-H₂O systems produced high surface area NPTs (156.9 m² g⁻¹) [85]. Meanwhile, the hydrothermal time and precursor ratio applied to NSTs can lead to different crystallinity, namely cubic, rhombohedral, and intergrowth of the two phases. Such intergrowth created a heterojunction between the In crystalline structures (e.g., InOOH/In₂O₃ and In(OH)₃/InOOH [86,87], thus presenting a new tool to form heterojunctions. The intergrowth narrows down the interfacial region to a few atomic scales, decreases the band bending, and produces less mismatch of their band structures to facilitate charge transfer.

Novel strategies for the formation of NSPs, and NRs calcining MOFs as sacrificial templates increased the surface area and the number of OV. The newly adapted synthesis method reached ~56 and ~48% PFOA defluorination in 8 h for the NSPs and NRs, respectively [88]. N-doping strategies of In₂O₃ demonstrated a PFOA defluorination rate of 36.1% in 6 h due to the redshift of the UV/Vis absorption spectrum, and

a bandgap reduction compared to its parent material [89]. The coupling of Fe salts and In₂O₃ enhanced the PFOA degradation by a factor of 3 due to the complexation of PFOA via Fe³⁺ and calcination ensured the catalyst stability. However, high temperatures (>400 °C) were unfavorable because the number of OV and surface area decreased [90].

2.4.2.2. Indium composites. The two main approaches to producing In composites are by 1) coupling In with carbonaceous materials, and 2) creating heterojunctions with different metals and metal oxides to form S-M and semiconductor-semiconductor (S-S) heterojunctions. Among the carbon-based photocatalysts, In₂O₃ NPs-graphene composite achieved over 60% defluorination of PFOA in 3 h. The addition of graphene in a small amount (2.5%) was beneficial for electron-hole separation due to the conductive graphene-layered structures which created an S-C heterojunction [91]. The low graphene content avoided significant semiconductor surface coverage, and heat treatment (400 °C) stabilized the material.

In recent years, a major trend is to couple In₂O₃ materials with other metals and metal oxides, such as Co₃O₄, NiO_x, and MnO_x to increase the number of OV in the material. Interestingly, MnO_x-In₂O₃ composite outperformed commercial In₂O₃ reaching 40% defluorination after 16 h, which represents a ~20% increase [92]. Under optimum Ce content, the CeO₂/In₂O₃ composite defluorinated over 50% PFOA in 1 h, due to the effective staggered gap heterojunction formation [93]. Coupling Pt with In₂O₃ NRs increased the PFOA degradation by over 35% in 1 h [94]. Quenching agent tests with benzoquinone, t-butyl alcohol, and KI, (for •O₂⁻, •OH, and h⁺, respectively) demonstrated a dual mechanism based on direct h⁺ oxidation and •O₂⁻ degradation. The Pt cost and the acidic pH emerges as drawbacks. In addition, low pH is generally undesirable, due to the need for chemical addition, and the potential leaching of ionic species.

2.4.3. Bismuth-based photocatalysts

Bismuth oxyhalide (BiOX) materials present high photocatalytic activity (Table 4). The spaced Bi₂O₂ layered structure polarizes the related halogen atom slabs and orbitals creating an electric field (Fig. 3A) that can prevent electron-hole recombination [95]. Different halides have been tested as BiOX materials for PFOA defluorination, but chloride and bromide exhibited the best performance. Besides the influence of the

Table 4

Summary of parameters for BiOX-based composites for PFOA defluorination (*combination of lamps).

Catalyst	Dose, g L ⁻¹	Pollutant, mg L ⁻¹	Power, W	pH	Time, h	Wavelength, nm	Removal, %	Defluorination %	Ref
BiOF	0.5	15	500	-	6	UV	> 99	26	[95]
In-MOF/BiOF	0.5	15	500	-	3	> 300	> 99	~34	[99]
BiOCl NST	0.5	8.28	10	4.8	24	254	> 99	59.3	[26]
BiOCl	1	20.70	300	3.9	8.5	> 300	~70	13	[104]
BiOCl	1	20	500	4	12	SS	> 99	~70	[100]
BiOCl	1	20	500	4	4	SS	> 90	29.93	[105]
BiOCl	0.05	20	32	3.8	1	254	> 99	> 55	[117]
BiPO ₄ /BiOCl	0.05	20	32	3.8	1	254	> 99	> 55	[117]
BiOCl NST	1	8.28	10	4.6	8	254	> 99	59.6	[106]
BiOCl NST	0.5	50	500	4	2	365	> 99	41.0	[102]
OV-BiOCl PPS	1	10	500	-	4	UV	> 99	~60	[107]
OV-BiOCl	1	10	125	-	2	~365	91.1	17	[103]
Zn-Al/ BiOCl	0.5	0.5	500	2	6	350-780	94	~32	[24]
BiOI@Bi ₅ O ₇ I	0.5	15	800	3	2	400-760	~80	-	[108]
Bi ₅ O ₇ I@ZnO	0.5	1	500	4	6	> 420	91	~40	[109]
Bi/BiOI _{0.8} F _{0.2}	0.4	40	800	5	3	SS	> 99	~10	[110]
BiO _{1.95} Br _{0.05}	0.4	20	300	-	2	> 400	> 99	-	[111]
BiOCl@TiO ₂	0.1	10	30	4.85	8	254	> 99	82	[113]
BiOBr@TiO ₂	0.1	10	30	4.85	8	254	96	65	[113]
BiOBr@TiO ₂	0.5	100	300	3.5	1.7	> 320	99.5	39.8	[114]
BiOI@TiO ₂	0.2	10	30	4.85	8	254	88	~20	[113]
Bi ₃ O(OH)(PO ₄) ₂	1.8	~54	18	4	2	254	> 99	> 60	[116]
Bi ₃ O(OH)(PO ₄) ₂	0.5	20	18	4.5	3	254	> 99	57.6	[118]
BiPO ₄	0.05	20	32	3.8	1	254	> 99	> 43	[117]
Pt-Bi ₂ O ₄	0.2	0.1	300	7	6	> 420	-	< 7	[34]
Bi ₂ O ₂ S	0.25	50	-	4	10	254	> 99	60.6	[120]
Bi ₂ O ₂ Se	0.25	50	-	8.17	10	254	> 99	54.2	[120]
Pb-BiFeO ₃ /rGO	0.1	50	5	2	8	254	69.6	37.6	[122]
BiOHP/CS	1	0.2	18	7	4	254	> 99	32.5	[123]

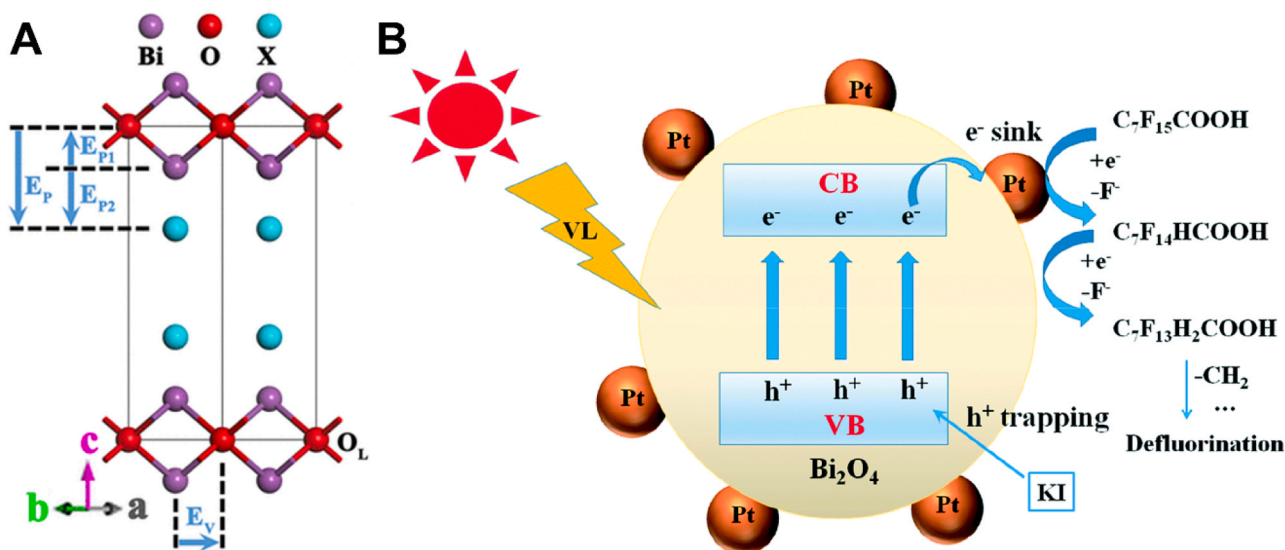


Fig. 3. A) BiOX built-in electric fields and atomic structure. EP denotes parallel to the normal direction of the Bi₂O₂ layer, which can be divided into two subfields. EV denotes that it is vertical to the normal direction of the Bi₂O₂ layer [101]; B) Pt-Bi₂O₄ photoreduction mechanism based on direct F⁻ extraction [34].

halide in VB modification [96,97], crystallinity control of the BiOX materials [98] allows the tunability of the facets, OVs, and bandgap, to enhance the PFOA defluorination. Additionally, other Bi-based materials, although less reported, are also effective in PFOA degradation (Table 4).

The halide in the Bi₂O₂ layer determines the nature and performance of these materials. In the synthesis of bismuth oxyfluoride (BiOF), ethylene glycol was introduced to populate the OVs and to increase the surface area of BiOF. The OVs provided stronger PFOA interaction and increased the light absorbance capacity, which enhanced the PFOA photodegradation [95]. The performance of BiOF was further enhanced by constructing a built-in electric field in In-MOF/BiOF, which

defluorinated up to 34% PFOA in 3 h. Theoretical calculations confirmed that pre-adsorption of PFOA is a key step in the photodegradation processes [99].

As the most common BiOX catalyst, the PZC of BiOCl is 2.8 [100] and thus the electrostatic attraction does not account for the adsorption of PFOA anions. Instead, the adsorption process is driven by the coordination of PFOA with the OVs to complex the carboxylic head of PFOA [100]. The PFOA defluorination by BiOCl is 1.7 and 14.6 times higher than In₂O₃ and TiO₂, respectively [26]. In addition, the h⁺-mediated oxidation is thermodynamically favored due to the positive oxidation potential of BiOCl (VB_{BiOCl} = 3.3 eV) compared with In₂O₃ (VB_{In2O3} = 2.8 eV) and TiO₂ (VB_{TiO2} = 3.2 eV) [26].

BiOCl can be tuned with preferential crystal facets to promote OVs for bidentate PFOA adsorption and enhanced photodegradation. For example, the PFOA degradation at the (010) facet was 2.64 times higher than that of the (001), due to the increased adsorption capacity (55.6–32.7 mg g⁻¹ h⁻¹ for 010 and 001, respectively) and decreased the adsorption energy (-0.265 eV for (001) to -0.399 eV for (010)) [102]. In addition, the oxygen atoms in [Bi₂O₂]²⁺ easily escape from the (010) facets due to the larger space compared to the (001) facet, which favors the e_{aq}^- capture [103]. These results highlight the importance of understanding the catalyst's structural properties to reach optimum catalytic properties.

The synthesis strategies also matter when increasing the OVs of BiOCl. Microwave solvothermal synthesis exhibited almost 3 times better defluorination rates for PFOA compared to precipitation and solvothermal methods [104]. Similarly, acetic acid was the solvent that achieved the highest separation rate of photo-induced charge pairs [105]. The alkaline source also affected the density of OVs following the order of (CO(NH₂)₂(0.573) < NH₃·H₂O(0.643) < NaOH(0.750) < Na₂CO₃(0.981)) [106]. The addition of modifiers, such as polyphenylene sulfide promotes the OVs formation, and enhances PFOA defluorination by ~40% after 4 h, compared to non-modified BiOCl [107].

Likewise, BiOBr and BiOI materials have formed heterojunctions with other BiOX materials and semiconductors. Among the most relevant materials, p-n BiOI@Bi₅O₇I [108] and n-n Bi₅O₇I@ZnO [109] exhibit high defluorination efficiencies. In addition, F was doped into a BiOI structure to decrease the bandgap of the individual material [110], while Br was doped into BiOI to promote the (001) crystal facet [111]. Recently, different BiOX/TiO₂ heterojunctions (X = Cl, Br, I) were synthesized and outperformed the pristine BiOX or TiO₂ due to the formation of a staggered bandgap structure [112]. BiOCl/TiO₂, BiOBr/TiO₂, and BiOI/TiO₂ defluorinated ~80, ~60, and ~20% of PFOA in 8 h, confirming BiOCl is among the best BiOX materials for PFOA defluorination under UVC [113]. Separate studies observed comparable results (~40% defluorination in 100 min) for BiOBr/TiO₂ even irradiating at 320–780 nm [114], suggesting the potential application of BiOX under solar light irradiation.

The high performance of BiOX materials also raised interest in other Bi-based materials targeting PFOA degradation. For example, Bi₃O(OH)(PO₄)₂ [115,116] and BiPO₄ showed over 60% PFOA defluorination in 2 h [116] and 40% in 1 h [117], respectively. Interestingly, photo-induced OVs at the surface of Bi₃O(OH)(PO₄)₂ [118], and the synthesis parameters [119] promoted the initial limiting decarboxylation step enhancing the PFOA degradation. Pt was also coupled with a novel hydrothermally synthesized Bi₂O₄ catalyst for PFOA photoreduction [36], where the direct F abstraction by an e_{aq}^- was realized under visible light due to the Pt atoms (Fig. 3B) [34]. Bi₂O₂S and Bi₂O₂Se materials could reach ~55% defluorination after 10 h without pH adjustment [120]. Noted that Bi₂O₂Se exhibits its highest performance at near-neutral pH, which is a practical advantage. To enhance PFOA adsorption and recovery, magnetic BiFeO₃/GO and Pb-BiFeO₃/rGO photocatalysts were prepared [121]. The latter photocatalyst defluorinated PFOA up to 37.6% in 8 h [122]. Similarly, the concentrate-and-destroy approach was also realized by combining bismuth phosphate (BiOHP) with modified carbon spheres (CS), which present complete PFOA removal (0.2 mg L⁻¹ PFOA with 1 g L⁻¹ catalyst) and crystalline structural stability after degradation compared to BiOHP [123].

The effective PFOA defluorination results from Bi-based materials justify their potential application in PFAS remediation, especially the BiOX. However, the charged nature of most Bi materials may be affected by the polarity and ionic species of the environment. Therefore, monitoring and reporting the structural stability, material recovery, and catalyst leaching is encouraged. In addition, the influence of ionic species and complex water matrixes should be systematically studied and discussed in-depth.

2.5. Emerging photocatalysts

This section summarizes and discusses new families of materials based on novel semiconductors (Table 5) aiming to improve the moderate performance of Ti-based materials, the practical limitations of homogeneous Fe ions, and the scarcity, and cost of the post-transition metal catalysts.

2.5.1. Silica-based materials

Silicon carbide (SiC) catalysts degrade PFOA due to their suitable CB position and the activation capacity of the C–F bonds. Graphene was coupled with SiC to enhance the availability of the e_{aq}^- [35]. The PFOA degradation rate constant of SiC/Graphene, and SiC were over 3 and 1.5 times higher than TiO₂. Besides, Pt atoms anchored on the surface of the SiC defluorinated 50.6% of PFOA due to the favored C–F bond activation and formation of a reactive Si–H bond. As a result, F is anchored at the surface of the silica due to hydrogen spillover from single atom Pt to SiC surface [37]. Given a synergy between the redox capabilities, high stability, and large surface area (896 m² g⁻¹), phosphotungstic acid bimodal mesoporous silica (HPW/BMS) composite achieved 3 times higher degradation rate (50% defluorination in 4 h) than direct VUV photolysis [124]. These works confirm the potential application of Si-based materials as effective adsorptive [73] and/or degrading materials for PFOA.

2.5.2. Boron nitride materials

Boron nitride (BN) is a novel high-performing photocatalyst with simple or no preparation requirements. A ball milling modification can induce defects on the BN material to enhance the PFOA degradation by ~20% and ~40% compared to commercial BN and TiO₂, respectively after 2 h [125]. Interestingly, when coupled with TiO₂, a novel composite degrades PFOA even under natural sunlight conditions with 68% defluorination after 7 h [126]. The band diagram indicates the formation of a staggered gap heterojunction, which promotes the role of photogenerated h^+ [126]. The leaching tests confirmed the stability of the materials and the sunlight irradiation facilitated its practical use in real water treatment applications. These results provide an alternative approach to integrating abundant and cost-effective TiO₂ to enhance the catalyst performance with simple synthesis methods.

2.5.3. Other photocatalysts

Recently, a novel diamond-based photocatalytic system avoided the chemical addition and pH dependence of sulfite-based e_{aq}^- production. The negative electron affinity of diamond promotes the electron emission into the aqueous phase to defluorinate PFOA (~60% in 3 h) with UV irradiation [33]. Higher PFOA defluorination (87.3% in 5 h at 45 °C) was observed by a core-shell CeO₂@NiAl double-layered hydroxide (LDHs) nanocomposite. The photocatalyst consisted of a z-scheme heterojunction, which accumulated h^+ in the VB of the CeO₂ and electrons in the CB of NiAl LDH [30]. The material's defluorination performance is attributed to the high surface area of LDHs and the extended visible light response and electropositivity of CeO₂. Meanwhile, a novel method for interlayer expansion of 2D titanium carbide (Ti₃C₂) MXene using deep eutectic solvents combined with hydrothermal preferential-facet TiO₂ growth promoted charge separation and PFOA defluorination. The composite defluorination was approximately 5 times more (49% in 16 h) than P25 in 24 h [127]. Despite the challenging synthesis of the layered structure, sensitive handling, and low structural stability emerging as MXene limitations [128], these works demonstrate the potential of MXenes and LDHs as photocatalytic materials.

3. What we know: evaluation of the materials

3.1. Performance evaluation

Chemical-free photocatalysis is a well-known technology in the

Table 5
Summary of parameters for other composites for PFOA defluorination. *see work for details.

Catalyst	Dose, g L ⁻¹	Pollutant, mg L ⁻¹	Power, W	pH	Time, h	Wavelength, nm	Removal, %	Defluorination %	Ref
SiC@Graphene	0.5	~50	5	7	6	254	~60	-	[35]
Pt-SiC	0.5	~50	5	7	1.5	254	> 95	50.6	[37]
BN	2.5	50	24	6.5	4	254	> 99	~52	[125]
BN@TiO ₂	0.5	50	24	3.2	7	SS	> 99	68	[126]
BN@TiO ₂	0.5	50	24	3.2	4	365	> 99	37	[126]
BN@TiO ₂	0.5	50	24	3.2	1	254	> 99	55	[126]
HPW/BMS	0.2	5	8	4	4	185 & 254	> 90	~50	[124]
CeO ₂ @NiAl-LDHs	0.5	50	500	9	5	400-800	90.2	87.3	[30]
Ti ₃ C ₂ /TiO ₂	0.2	8.28	-	3	16	UV	> 99	49	[127]
Diamond	*	8.28	500	7	3	UV	> 99	~60	[33]

catalysis community, yet there is a lack of comparison among published works on the performance and the economic viability of the materials. Among the number of operational parameters involved in PFOA photocatalytic degradation, the initial concentration, non-neutral pH conditions, and defluorination profiles are key parameters to describe photocatalysts' performance in water treatment to mimic real water conditions and ensure near-zero fluoropollution. However, they are

often omitted arbitrarily selected, which challenges their comparison and demonstrates the need to establish relevant parameters to accurately describe the photocatalysts' performance.

Our analysis of the current literature captured the lack of comprehensive material characterization and the overlooked operational parameters. Specifically, a few works reported on the photon flux, the fluence dosed, the leaching of the materials, the pH stability, types of

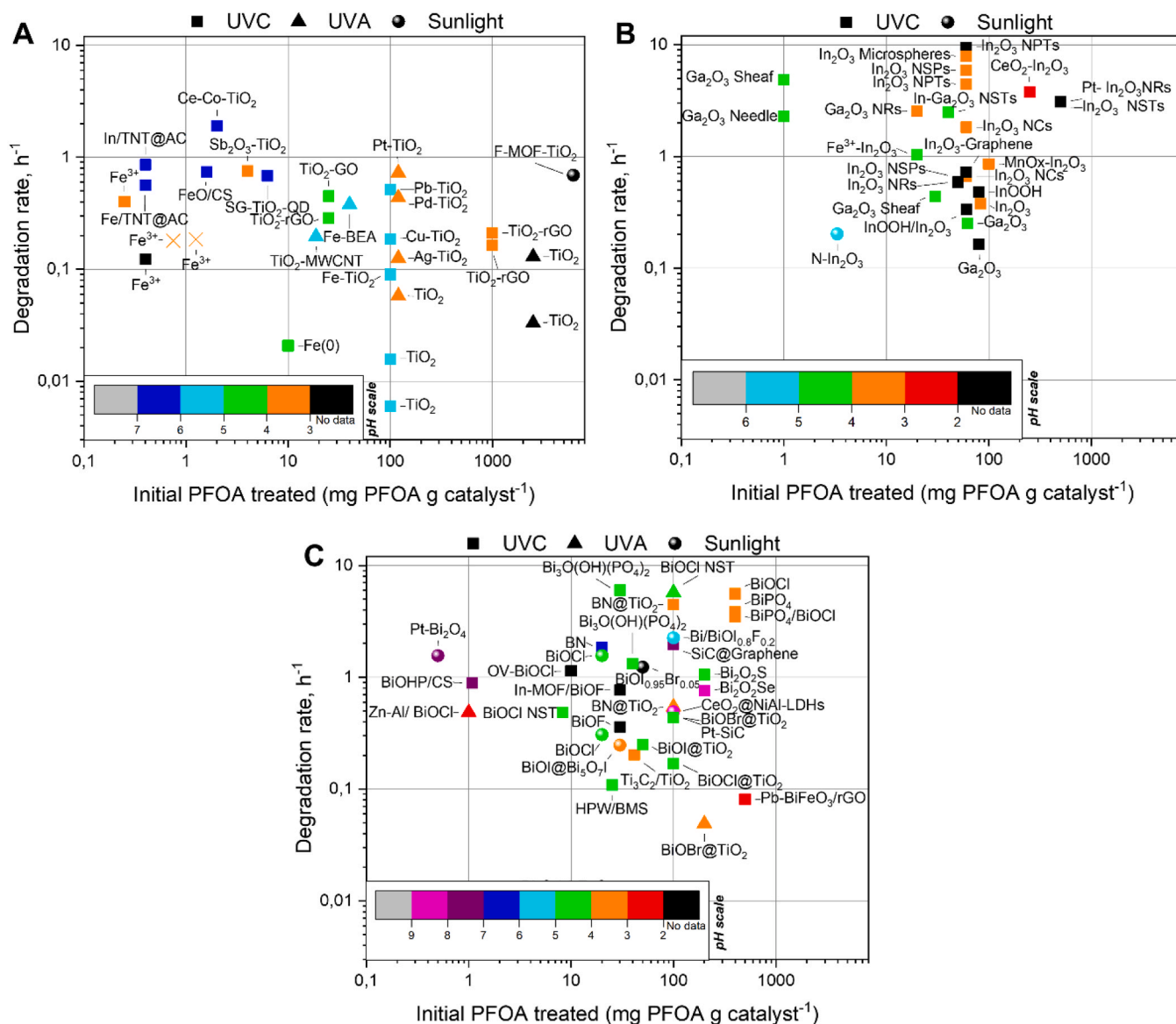


Fig. 4. Map of the reported PFOA treatment efficiency of different chemical-free photocatalytic materials: A) Titanium and Iron-based materials, B) Indium and gallium-based materials, and C) Bismuth and novel materials. The (x) symbol refers to VUV irradiation.

irradiations, and the effect of complex water matrixes, which hinder a fully reliable and constructive comparison. Particularly, organic matters and inorganic ions' interaction with RS, such as h^+ or e_{aq}^- , may result in materials underperformance. Fig. 4 compares the chemical-free photocatalysts in terms of practical (PFOA concentration, pH), energy demanding (irradiation wavelength) and performance (degradation rate) perspective, based on the most available data in publications. It can be noted that photocatalysts operate under a wide range (10^4 - 10^5 mg g^{-1}) of concentrations, further discussion on the application of concentration technologies, specific contamination sites, or analytical limitations is needed to justify the initial concentrations. Moreover, the materials tend to work under acidic conditions and just a small fraction operate in neutral environments (e.g., dark blue, purple). TiO₂ and Fe-based (Fig. 4A) materials tend to underperform In/Ga-based materials (Fig. 4B), and Bi-based and novel photocatalysts (Fig. 4C), while some of these catalysts present higher degradation performance compared to TiO₂, they rarely exhibit optimum performance at near-neutral pH.

Moreover, degradation and defluorination are not the only important parameters identifying performance. Parameters such as stability, cost, and energy input are important for the application of photocatalysts. Table 6 shows – based on the criteria described in Text S2 – practical considerations for the application of photocatalysts in water treatment applications, in which ease of synthesis, chemical stability, type of wavelength, quantum efficiency, optimum pH, and cost are considered. This critical and wholistic overview allows for identifying both promising options for PFOA treatment as well as capturing areas for further improvements. For example, Ti-based materials have been implemented in combination with other semiconductors or carbon materials. Yet, their performance remains modest even under optimum non-realistic conditions. Similarly, Fe-based materials are attractive due to their

low-cost, but their homogenous catalysis chemistry and acidic pH requirements challenge their recovery and practical application. The post-transition metal In₂O₃ and Ga₂O₃ photocatalysts present slightly better degradation performance, yet their high cost limits their implementation for bulk water treatments. Indeed, novel materials such as SiC, BN, and Fe-BEA zeolite present practical advantages (i.e., pH dependency, negligible secondary pollution, and low-energetic wavelengths), which drive photocatalysis a step forward to its application for PFOA treatment. Accordingly, research on novel photocatalytic materials should first aim to focus on the defluorination efficiency of the materials, which is often underreported, and it is essential to avoid releasing short-chain PFAS byproducts. It is also essential to overcome the practical limitations of the materials, as discussed for the novel photocatalysts, to apply the material under realistic water conditions (e.g., pH, salinity).

3.2. Mechanistic degradation

Based on the current literature, we identified that h^+ and e_{aq}^- are the main RS initiating the PFOA degradation processes (Fig. 5). Despite mechanism descriptions rarely involving reaction sites (i.e., catalyst surface or solution), h^+ -oxidation of anionic PFOA forms unstable intermediate radicals that undergo decarboxylation to form short-chain PFCAs, $\bullet OH$ and $\bullet O_2^-$ can further accelerate the degradation. Similarly, Fe ions present PFOA complexation properties, which allow the electron transfer from the PFOA to Fe³⁺ in an LMCT mechanism to form unstable radicals as occurring in h^+ -oxidation. A plausible degradation model involves a four-step process named decarboxylation–hydroxylation–elimination–hydrolysis, which is common in both initiation mechanisms in Fig. 5. Similarly, e_{aq}^- reduction is reported to undergo two main mechanisms, named attack the alcohol termination

Table 6

Summary of the relative practical performances of the main families of photocatalysts according to Text S2.

Material	Examples	Degradation rate	Defluorination extent	Ease of Synthesis	Chemical stability	Irradiation type	Quantum efficiency	pH	Cost	References
TiO ₂ @Carbon	C= GO, rGO, MWCNT, SGA	↓	↓	↓	?	↑	×	A	\$	[43,44,46–48,55,61,62,131,142]
M-TiO ₂	M=Fe, Cu, Pb, Pd, Pt	↓	↓	↓	?	↓	×	A	\$	[43,44,46]
Fe ³⁺	Fe ³⁺	↓	↓	↑	↓	↓	×	A	\$	[41,68,70,71]
In ₂ O ₃ , Ga ₂ O ₃	In ₂ O ₃ , NCs, NPs, NRs, Ga ₂ O ₃	↓	↓	↓	?	↓	×	A	\$\$	[42,76,77,83,88]
Nano In/Ga oxides	Needle, sheaf, NRs, NSTs, NSPs	↑	↑	↓	↓	↓	✓	A	\$\$	[79–81,83,91,93]
In/Ga composites	Fe ³⁺ , CeO ₂	↑	↑	↓	↓	↓	✓	A	\$\$	[79–81,83,91,93]
BiOX	BiOCl, NST,	↑	↑	↓	?	↑↑	×	A	\$	[102,105–107]
Bi catalysts	BiPO ₄ , TiO ₂ , In-MOF,	↑	↑	↓	?	↑↑	×	A	\$	[99,114,116–118]
	Bi ₃ O(OH)(PO ₄) ₂	↑	↑	↓	?	↓	×	A	\$\$	[116]
	Pt-SiC	↑	↑	↓	?	↓	✓	✓	\$\$\$	[37]
	Fe@Zeolite	↑	↑	↑	?	↑	✓	A	\$	[73]
	BN materials	↑	↑	↑	↑	↑↑	✓	A	\$	[125,126]
	HPW/BMS	↑	↑	↓	?	↓	×	A	\$	[124]
	CeO ₂ @NiAl-LDHs	↑	↑	↓	?	↑↑	×	B	\$	[30]
	Ti ₃ C ₂ /TiO ₂	↑	↑	↓	?	↓	×	?	\$	[127]
	C _{diamond}	↑	↑	↓	?	?	✓	✓	\$\$\$	[33]

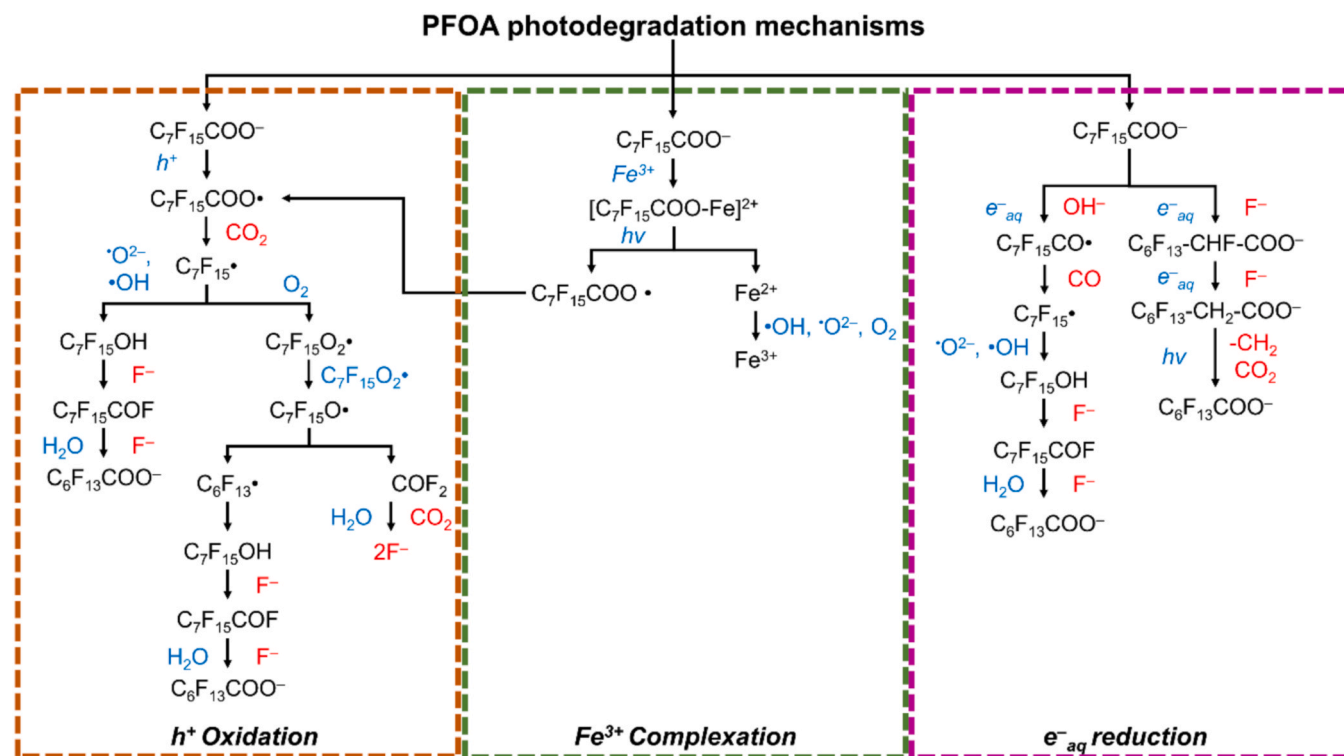


Fig. 5. Proposed initiating chemical-free photodegradation mechanisms for PFOA degradation based on h⁺ oxidation, Fe³⁺ complexation, and e_{aq}⁻ reduction [26,30,34,35,41]. This image does not include activated systems where •O₂⁻ or ¹O₂ may initiate the degradation.

or directly attack the C-F bond.

3.3. Techno-economic evaluation

The current proposed regulatory limits highlight the importance of identifying cost-effective methods that can reliably destroy PFAS down to the ng/L range. It is therefore imperative for the photocatalysis research community to determine the viability of applying photocatalysis to meet these requirements. Thus, we argue that significant focus is needed to cover innovative reactor designs and techno-economic analysis (TEA) to move PFOA photocatalytic research to real-world applications. TEA is a critical step to ensure the feasibility of the materials and technology as medium and large-scale processes. Unfortunately, academic articles rarely present enough information on the catalyst synthesis cost or process energy requirements to directly compare materials. Besides, the activity parameters are not uniformly presented in publications. For example, defluorination kinetics and irradiation parameters are essential benchmarks often omitted.

Accounting for these limitations, we designed a TEA model (additional details in **Text S1a**, **Fig. S1**). To compare the effectiveness of representative catalysts (**Fig. S2**) described in this review, we calculated two metrics (**Table S4**): the defluorination output (**Text S1b**) and the operational cost of technology (**Text S1c**). Despite the limitations of the TEA model (e.g., variable materials and energy price), this novel tool can describe general trends for each family and highlight the need to report costs for effective materials comparison. For example, TiO₂ materials have a low price (below \$1.5) and low defluorination output but they can enhance their performance when paired with other materials. Materials such as some M-TiO₂ and BN@TiO₂ have substantially better performance without a significant increase in cost. An interesting trend is observed coupling BN and TiO₂ compared to BN alone. The novel heterojunction formation promotes the price decrease of the material while increasing its performance. Conversely, coupling rare metals to semiconductors increase the cost of the composite formation (i.e., Pd-TiO₂) and challenges its practical application, while common metals (e.

g., Fe) are more cost-effective. Its abundance and spread are used to make it a suitable candidate, despite the defluorination performance, remaining modest. Additionally, the opportunities to improve this material are limited.

The performance of post-transition metal-based catalysts was reported in previous studies [19] and confirmed by our model. These materials outperform Ti-based materials due to their band positions and enhanced adsorption properties. In addition, surface geometry modification produces higher reactivity. Our model suggests that modifying In and Ga catalysts can enhance the defluorination output but often require more operational costs. Further studies are encouraged to determine these benefits. Bismuth-based catalysts outperform the In and Ga-based materials in terms of cost, despite their typically moderate performance. Surprisingly, Bi₃O(OH)(PO₄)₂ outperforms in terms of degradation and its price is in an intermediate range based on our estimations (\$1.5/g to \$3/g). The bidentate adsorption of the catalyst and the fast defluorination kinetics of the catalyst results in a high defluorination output. Novel materials overperform TiO₂, but they fall under the low-price, low-performance category. Therefore, post-transition metal-based catalysts tend to outperform Ti semiconductors and novel catalysts. However, this TEA analysis focuses on the defluorination outcome, and it effectively excludes other benefits and strategies summarized in **Table 6**, which are essential for the practical application of the technology.

4. Where we go from here: perspectives and research lines

Many studies have reported that photocatalysts can achieve complete degradation of PFOA under different initial concentrations, irradiation wavelengths, and pH values in hours. However, complete defluorination of any PFAS is still challenging and drawbacks associated with the technology are present. This section summarizes the main challenges related to the performance, which are associated with the effective charging separation and surface properties, and the scale-up evaluations, which are related to the irradiation parameters, the stability of the materials, and the concentration of the streams. We also

provide perspectives on the technology development for enhanced photocatalytic defluorination of PFOA and other PFAS.

4.1. Charge separation

Effective charge separation is essential for producing RS to improve PFOA degradation. The most common strategy to enhance the charge carrier's lifetime is to form a heterojunction. From the materials perspective, we identified are 4 main types of heterojunctions to deal with PFOA: S-S [93,126], S-M [34,36,37], S-C [55,91], and multi-component heterojunctions of more than two materials in a composite [56,129]. The most fabricated heterojunctions used in PFOA degradation are S-S and S-C heterojunctions. Heterojunctions can also be classified into non-p-n [57] and p-n [130] heterojunctions depending on the electronic density of the materials. The different electronic density of p- and n-semiconductors is determined by the lack and excess of electrons in the crystalline structure, respectively. The formation of a p-n heterojunction creates an electric field that favors the diffusion of electrons from the n-semiconductor to the p-semiconductor, and the other way for the h^+ [112]. This charge separation process prolongs RS lifetime for PFOA degradation.

The S-S heterojunction result from the interface between two different semiconductors with unequal band structures. Based on their band alignment, there are three types of heterojunctions (Fig. 6). In Fig. 6A electrons and h^+ are accumulated in semiconductor 2 resulting in inefficient charge separation. Fig. 6B represents the staggered gap, which is the most effective system to enhance photocatalytic performance. The photogenerated electrons are transferred to semiconductor 2 and h^+ are transferred to semiconductor 1 for efficient charge separation. In Fig. 6C the bands do not overlap, therefore charge separation cannot occur. Additionally, z-scheme heterojunctions are a different type that relies on an electron donor/acceptor pair to migrate the electron between two semiconductors [30,112].

The material design is a critical step to produce effective heterojunctions and promote charge separation for PFOA degradation. As for the S-C heterojunctions, graphene [62] and rGO [122,131] could decrease electron-hole recombination because of their electron-trapping capacity. Identifying the effective RS is essential to understand the reaction mechanisms and limitations of the photocatalytic materials. Therefore, determining the semiconductor's band diagrams is essential, and often omitted, for mechanistic understanding in novel photocatalytic materials and composites. Further, characterization of the components, and the type of heterojunction, can shed light on the VB and CB positions, which are critical to determining the oxidative potential of the RS that plays a role in the PFOA degradation process. For example, the S-M heterojunction relies on conductive metals such as Pt [36], Ag, or Pd [46] to trap photogenerated electrons [36], reduce the bandgap or extend the h^+ lifetime to degrade PFOA [46]. However, heterojunctions can also be preferentially produced to improve the

PFOA adsorption and promote the reactivity of the RS, as occurs with carbon nanotubes [55] or AC [58].

4.2. Surface structure

The absorption spectrum of photocatalysts depends on the structure and composition of a material. Modifying the optical properties to visible light can improve the energy efficiency in PFOA photodegradation. The optical properties have typically been modified by three different strategies. First, doping the structure to alter the order of a crystal and create structural (i.e., atomic substitution [45,110]), and surface defects (i.e., OV [95,100,102,103]). Second, annealing treatments change the crystalline structure by altering either the crystallite size or the crystalline phase [132,133]. Third, reducing the material to the nanoscale, so that the density of states in the CB [134] shifts the absorption spectrum to blue and increases the energy required to excite the electron. Since nanocatalysts have enhanced optical and structural properties and exhibited higher adsorption capacity, many photocatalyst morphologies were nanoengineered, including tubes [55], dots [64], spheres [83], flower-like shapes [109] in 1D to 3D dimensional structures [64,86,110], along with various crystal facets. The absorption range, bands, and adsorption capacity can also be modified by understanding and tuning the catalyst structure. Fundamental research on the crystallography, structural information, and mechanistic interaction of the materials with PFOA provide insights to enhance the degradation and design of novel materials. In addition, this research broadens the application spectra of the materials to other fields (i.e. antibacterial coatings, water splitting, or self-cleaning functions).

4.3. Photocatalyst irradiation

4.3.1. Irradiation wavelength

PFOA can be directly degraded and defluorinated below 200 nm [41] because the irradiation promotes the initial decarboxylation step. Most photocatalysts for PFOA degradation operate in intermediate UV regions of 200–400 nm. In this context, efforts are encouraged to research solar-driven PFOA photocatalysts [108,126]. The usage of solar-active outdoor photocatalysts can reduce the costs related to reactor design and energy consumption, and it can enhance the safety of the overall process [135]. However, the interrupted and seasonal availability of solar light prevents the continuous and effective use of this energy source. Therefore, photocatalysis research is not only limited to material development but also to technological advances to minimize the use of external photoreactors, maximize the photon flux, and ensure continuous flow, which are practical advantages to drive the PFOA degradation one-step forward to the near-zero discharge goal.

4.3.2. Reactor design

The reactor design is critical, especially when scaling up the

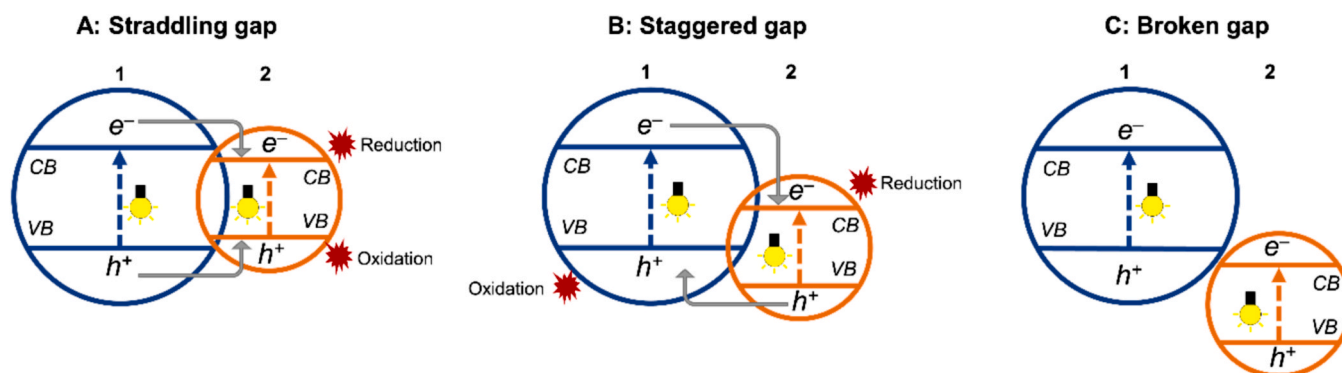


Fig. 6. Types of non-p-n heterojunctions A) accumulation of charges, B) effective charge separation, C) no charge separation.

technology [136,137], to understand the influence of operational parameters such as incident irradiation, light distribution, energy usage, and aeration needs [138,139]. Research currently focuses on the development of mechanistic and novel materials rather than novel photoreactor configurations for real water treatment applications. The lack of applicable reactor designs challenges the practical implementation of photocatalytic technologies in PFAS remediation. It is strongly recommended that current research progressively turns the focus from the lab to the pilot scale. Few studies report PFOA treatment in continuous flow reactors which might be a simple solution to scaling up the technology. However, the continuous operation might require additional technologies (i.e., membranes) and treatment of the separated catalyst slurry. In this context, immobilization of the photocatalyst on the reactor wall [140] may overcome the drawback. However, it may decrease the light penetration and catalyst efficiency.

At the lab scale, the irradiation surface and its distance from the emitting source affect the irradiation treatment. Short distances can increase the light intensity, but the homogeneity of the irradiation decreases [141]. Mixing is effective to increase the interaction between PFOA and catalysts, ensuring the homogeneity of the system and preventing particle settling and screening [142]. In fact, each material presents an optimum dose, which has to be considered to scale up the process [138]. In addition, instrument materials adsorbing PFOA could result in misleading results [143]. Therefore, it is critical to report and confirm the adsorption of the materials employed during the experimental process. The reactor material is also related to the irradiation wavelength because it only transmits certain wavelengths. For example, heterogeneous photocatalysts operating at 254 nm require quartz reactors to prevent light absorption. Further research in this field is needed to develop effective materials, normalize the results, and establish reliable methods to compare state-of-the-art reactors. The fabrication and utilization of those materials are important considerations for large-scale reactors.

4.4. Recovery, leaching, and reusability of catalysts

The recovery of photocatalysts in water treatment applications is a practical concern. The need to develop nanoscale materials to achieve high removal efficiency challenges its recovery [144]. The catalyst coupling with separation technologies, such as membranes, emerges as an alternative to AC adsorption and ion-exchange resins [145]. Nevertheless, fouling, insufficient separation, and membrane lifetime [146, 147] often challenge the membrane application for non-pure streams and large water bodies. In this context, engineering porous micro-sized materials with high surface area and settling properties can facilitate recovery [144], but separation from water is still required. The development of magnetic materials is an alternative separation strategy [148]. For example, anchoring the photocatalyst onto magnetic reactor walls with an external magnetic force to limit the manipulation and facilitate the recovery.

In addition, the leaching of the materials must be minimized to meet the discharge regulations and ensure water quality. Effective bonding of photocatalytic materials has been achieved by different methods (i.e., hydrothermal [56,81], sol-gel [45,55], calcination [56,90,132]), but any leaching must be monitored. Additionally, morphology changes during the process can also shed light on the catalyst stability. The reusability tests are an indicator of the catalyst stability that is often not accurately assessed since the catalyst lost is not specified (e.g., material attached to the reactor walls). The reusability of the material can be monitored by spiking pollutants in the reaction solution after each degradation cycle, while the recovery can be reported as the mass of material recovered after each cycle.

4.5. Treatment of low-concentrated streams

Due to their typically low concentration, the design of adsorptive

composite materials concentrates PFOA and promotes its reactivity with active RS [21,58,74]. In general, the mechanism of PFOA adsorption mainly relies on (I) electrostatic interactions with charged groups on the adsorbent, (II) hydrophobic interactions between the adsorbent and PFOA molecules, and (III) physical constraining by morphology and porosity of the adsorbent.

The concentrate-and-destroy approach provides a new perspective for remediating low-concentration PFOA. There are four main strategies to improve the adsorption and reaction at the composite surface. First, coupling a photocatalyst with a sorbent material (i.e., AC [56], graphene [142,149], zeolite [73], MOFs [150]). Second, tuning the functional groups of the material to selectively target PFOA. For example, positively charged functional groups, such as amine [151], are favored to attract the negatively charged PFOA [152]. Third, increasing the surface area and creating defects (i.e., OV) in the photocatalyst to create active sites for the PFOA to react. Fourth, doping the photocatalyst with a more surface-positive material (i.e. metal oxide [56], single-atom doping [37]) to displace the PZC of the composite and enhance the PFOA adsorption.

Specifically, Liu et al. reported a TNT@AC composite capable to concentrate-and-destroy phenanthrene by removing 90% of the initial volume [153]. The doping of this base material with different metal oxides (Fig. 7) such as Fe [56,154], In [57], and Ga [58] is effective for PFAS defluorination. The addition of these metals allows the shift of the PZC of the material favoring PFOA adsorption. In addition, their PFOA bidentate adsorption mechanism, and the produced heterojunctions provide an extra path for PFOA degradation (Fig. 2b). Similar types of materials are also successful in PFAS treatment, such as iron oxides [74] and BiOHP [123] loaded onto CS or zeolites [73].

Despite those obvious advantages, the usage of rare and expensive materials, the time required for the material to settle, the selective adsorption, and the catalyst separation and leaching may emerge as concerns for the practical application of the concentrate-and-destroy strategy. In addition, WWTP and industrial processes operate in a continuous flow, which requires a process modification to integrate the concentrate-and-destroy concept. In this context, the combination of membrane processes (i.e., microfiltration[144] or ultrafiltration[155]) with photocatalytic technologies have been commercially used for slurry-based photocatalytic systems, for enhanced recovery of adsorptive photocatalysts [156,157]. Photocatalytic membrane reactors have also been produced to concentrate and destroy micropollutants in-situ [146,156,158] which can be extended to PFOA degradation.

5. Conclusions

In this review, we provide a critical overview of the state-of-the-art photocatalytic materials for PFOA treatment. We summarize the main families of photocatalysts for PFOA degradation (Ti, Fe, Ga, In, Bi, Si, and BN), and discuss their strengths, drawbacks, and perspectives to address the needs of the technology. To date, many different catalysts, synthesis methods, and strategies have been tested, yet byproducts will be released in the reaction solution due to incomplete defluorination. To

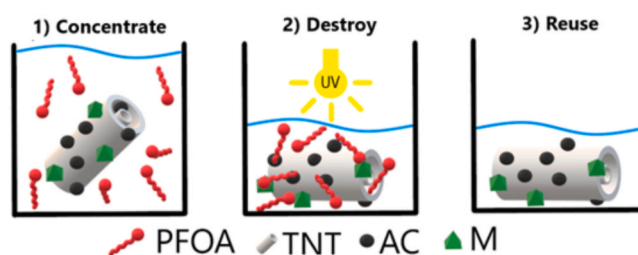


Fig. 7. Scheme of the concentrate-and-destroy strategy of a TNT@AC-based composite material. The green shape corresponds to the doping agent, which can be in the form of a metal or a metal oxide material.

further enhance the performance and practical usage of photocatalysts, the following key directions are suggested.

- Zero discharge of per- and polyfluoroalkyl substances (PFAS) is a crucial objective, and efforts must be directed toward the design of materials that can achieve this goal. The focus of material design should be on (I) effective adsorption of PFOA and short-chain PFAS; (II) development of effective heterojunctions (i.e., type B and p-n) and electron trapping strategies (i.e., Pt, and graphene) to enhance the lifetime of the RS and the defluorination kinetics; (III) production of sufficient RS capable of degrading PFOA using facet-engineering and crystal phase tuning.
- For the practical application of this technology at full scale, it is essential to develop engineering strategies that can work with large-scale water volumes. Therefore, it is critical to produce simple and cost-effective materials, develop solar-driven catalysts, and recover the material.
- The integration of photocatalysis with emerging and established technologies such as filtration, ion exchange, or adsorption is a research direction that can further improve PFOA treatments and overcome the limitations of single-treatment technologies.
- Understanding the effects of ions, organic matter, and coexisting species in complex water matrices on PFOA degradation at both lab and pilot scales is important. Coexisting species also include non-PFAS micropollutants such as pesticides, phenols, industrial chemicals, or pharmaceuticals.
- Optimizing the synthesis methods and utilizing green, simple, and stable materials is recommended to produce feasible and cost-effective catalysts. It is critical to report the leaching and recovery of the material before every reuse to determine stability and ensure no secondary pollution.
- At present, the available information published in the literature is insufficient to perform an accurate TEA of the catalysts required to homogenize the reporting parameters. Therefore, it is essential to perform economical evaluations of the costs of materials, implementation of the technology, operational costs, energy consumption, and further treatments at both lab and large scale.

Declaration of Competing Interest

The authors declare that they have no known competing financial interests or personal relationships that could have appeared to influence the work reported in this paper.

Data availability

No data was used for the research described in the article.

Acknowledgments

This work was supported by Aarhus University Centre for Water Technology (AU-WATEC) Start-Up Fund from Grundfos Foundation, Aarhus University Research Foundation Starting Grant (No. AUFF-E-2019-7-28), Novo Nordisk Fonden (No. NNF20OC0064799), and Independent Research Fund Denmark (No. 1127-00181B and Sapere Aude Award No. 1051-00058B).

Statement – Chemical-Free PFOA Degradation – What we know and where we go from here?

The growing concerns about PFAS have motivated research into cost-effective methods to prevent their release into the environment. Photocatalytic degradation, chemical-free process utilizing light energy, has garnered increasing interest for PFAS remediation in recent years. However, numerous novel photocatalytic materials and overlooked experimental parameters make systematic comparison between

materials challenging. This work categorizes and compares photocatalytic materials by composition-based families. Focusing on PFOA, key practical characteristics of the materials are identified (e.g. optimal pH, stability, defluorination capacity, cost) to elucidate promising research avenues. Generation of reliable, comparable data is critical for advancing photocatalytic technology development and scale-up for PFAS remediation.

Appendix A. Supporting information

Supplementary data associated with this article can be found in the online version at [doi:10.1016/j.jhazmat.2023.132651](https://doi.org/10.1016/j.jhazmat.2023.132651).

References

- [1] Post, G.B., Cohn, P.D., Cooper, K.R., 2012. Perfluorooctanoic acid (PFOA), an emerging drinking water contaminant: A critical review of recent literature. *Environ Res* 116, 93–117. <https://doi.org/10.1016/j.envres.2012.03.007>.
- [2] Sinclair, G.M., Long, S.M., Jones, O.A.H., 2020. What are the effects of PFAS exposure at environmentally relevant concentrations? *Chemosphere* 258, 127340. <https://doi.org/10.1016/j.chemosphere.2020.127340>.
- [3] Gagliano, E., Sgroi, M., Falciglia, P.P., Vagliasindi, F.G.A., Roccaro, P., 2020. Removal of poly- and perfluoroalkyl substances (PFAS) from water by adsorption: Role of PFAS chain length, effect of organic matter and challenges in adsorbent regeneration. *Water Res* 171, 115381. <https://doi.org/10.1016/j.watres.2019.115381>.
- [4] Li, F., Duan, J., Tian, S., Ji, H., Zhu, Y., Wei, Z., Zhao, D., 2020. Short-chain per- and polyfluoroalkyl substances in aquatic systems: Occurrence, impacts and treatment. *Chem Eng J* 380. <https://doi.org/10.1016/j.cej.2019.122506>.
- [5] Xu, Y., Fletcher, T., Pineda, D., Lindh, C.H., Nilsson, C., Glynn, A., Vogts, C., Norström, K., Lilja, K., Jakobsson, K., Li, Y., 2020. Serum half-lives for short- and long-chain perfluoroalkyl acids after ceasing exposure from drinking water contaminated by firefighting foam. *Environ Health Perspect* 128, 1–11. <https://doi.org/10.1289/EHP6785>.
- [6] Das, S., Ray, N.M., Wan, J., Khan, A., Chakraborty, T., Ray, M.B., 2017. Micropollutants in wastewater: Fate and removal processes. *Phys-Chem Wastewater Treat Resour Recover* 1–33. <https://doi.org/10.5772/65644>.
- [7] Luo, Y., Guo, W., Hao, H., Duc, L., Ibney, F., Zhang, J., Liang, S., Wang, X.C., 2014. A review on the occurrence of micropollutants in the aquatic environment and their fate and removal during wastewater treatment. *Sci Total Environ* 473–474, 619–641. <https://doi.org/10.1016/j.scitotenv.2013.12.065>.
- [8] Yamashita, N., Taniyasu, S., Petrick, G., Wei, S., Gamo, T., Lam, P.K.S., Kannan, K., 2008. Perfluorinated acids as novel chemical tracers of global circulation of ocean waters. *Chemosphere* 70, 1247–1255. <https://doi.org/10.1016/j.chemosphere.2007.07.079>.
- [9] Burch, K.D., Han, B., 2019. Removal efficiency of commonly prescribed antibiotics via tertiary wastewater treatment. *Environ Sci Pollut Res* 26, 6301–6310. <https://doi.org/10.1007/s11356-019-04170-w>.
- [10] U.S. EPA, Proposed PFAS national primary drinking water regulation, Per-Polyfluoroalkyl Subst., 2023. <https://www.epa.gov/sdwa/and-polyfluoroalkyl-substances-pfas> (accessed April 2, 2023).
- [11] European Chemicals Agency, 2021. How are PFASs regulated in the EU? Perfluoroalkyl-Contain Chem. (<https://echa.europa.eu/nl/hot-topics/perfluoroalkyl-chemicals-pfas>) (accessed April 2, 2023).
- [12] European Chemicals Agency, Considered restrictions, ECHA Publ. PFAS Restrict. Propos., 2023. <https://echa.europa.eu/nl/restrictions-under-consideration/-/substance-rev/72301/term> (accessed April 2, 2023).
- [13] Arana Juve, J.-M., Wang, B., Wong, M.S., Ateia, M., Wei, Z., 2023. Complete defluorination of per- and polyfluoroalkyl substances — dream or reality. *Curr Opin Chem Eng* 41, 100943. <https://doi.org/10.1016/j.coche.2023.100943>.
- [14] Leung, S.C.E., Shukla, P., Chen, D., Eftekhari, E., An, H., Zare, F., Ghasemi, N., Zhang, D., Nguyen, N.T., Li, Q., 2022. Emerging technologies for PFOS/PFOA degradation and removal: A review. *Sci Total Environ* 827, 153669. <https://doi.org/10.1016/j.scitotenv.2022.153669>.
- [15] Biswas, S., Yamijala, S.S.R.K.C., Wong, B.M., 2022. Degradation of per- and polyfluoroalkyl substances with hydrated electrons: A new mechanism from first-principles calculations. *Environ Sci Technol* 56, 8167–8175. <https://doi.org/10.1021/acs.est.2c01469>.
- [16] Román Santiago, A., Yin, S., Elbert, J., Lee, J., Shukla, D., Su, X., 2023. Imparting selective fluorophilic interactions in redox copolymers for the electrochemically mediated capture of short-chain perfluoroalkyl substances. *J Am Chem Soc* 145, 9508–9519. <https://doi.org/10.1021/jacs.2c10963>.
- [17] Lenka, S.P., Kah, M., Padhye, L.P., 2023. Losses of ultrashort- and short-chain PFAS to polypropylene materials. *ACS ES T Water*. <https://doi.org/10.1021/acestwater.3c00191>.
- [18] Mantripragada, S., Obare, S.O., Zhang, L., 2022. Addressing short-chain PFAS contamination in water with nanofibrous adsorbent/filter material from electrospinning. *Acc Chem Res*. <https://doi.org/10.1021/acs.accounts.2c00591>.
- [19] Xu, B., Boshir, M., Zhou, J.L., Altaee, A., Wu, M., 2017. Photocatalytic removal of perfluoroalkyl substances from water and wastewater: Mechanism, kinetics and controlling factors. *Chemosphere* 189, 717–729. <https://doi.org/10.1016/j.chemosphere.2017.09.110>.

- [20] Liu, F., Guan, X., Xiao, F., 2022. Photodegradation of per- and polyfluoroalkyl substances in water: A review of fundamentals and applications. *J Hazard Mater* 439, 129580. <https://doi.org/10.1016/j.jhazmat.2022.129580>.
- [21] Javed, H., Metz, J., Eraslan, T.C., Mathieu, J., Wang, B., Wu, G., Tsai, A., Wong, M.S., Alvarez, P.J.J., 2020. Discerning the relevance of superoxide in PFOA degradation. *Environ Sci Technol Lett* 7, 653–658. <https://doi.org/10.1021/acs.estlett.0c00505>.
- [22] Zhang, W., Efstathiadis, H., Li, L., Liang, Y., 2020. Environmental factors affecting degradation of perfluorooctanoic acid (PFOA) by In₂O₃ nanoparticles. *J Environ Sci (China)* 93, 48–56. <https://doi.org/10.1016/j.jes.2020.02.028>.
- [23] Kutsuna, S., Nagaoka, Y., Takeuchi, K., Hori, H., 2006. TiO₂-induced heterogeneous photodegradation of a fluorotelomer alcohol in air. *Environ Sci Technol* 40, 6824–6829. <https://doi.org/10.1021/es060852k>.
- [24] Yang, Y., Zheng, Z., Yang, M., Chen, J., Li, C., Zhang, C., Zhang, X., 2020. In-situ fabrication of a spherical-shaped Zn-Al hydroxalcalite with BiOCl and study on its enhanced photocatalytic mechanism for perfluorooctanoic acid removal performed with a response surface methodology. *J Hazard Mater* 399, 123070. <https://doi.org/10.1016/j.jhazmat.2020.123070>.
- [25] Chen, Y., Bhati, M., Walls, B.W., Wang, B., Wong, M.S., Senftle, T.P., 2022. Mechanistic insight into the photo-oxidation of perfluorocarboxylic acid over boron nitride. *Environ Sci Technol* 56, 8942–8952. <https://doi.org/10.1021/acs.est.2c01637>.
- [26] Song, Z., Dong, X., Wang, N., Zhu, L., Luo, Z., Fang, J., Xiong, C., 2017. Efficient photocatalytic defluorination of perfluorooctanoic acid over BiOCl nanosheets via a hole direct oxidation mechanism. *Chem Eng J* 317, 925–934. <https://doi.org/10.1016/j.cej.2017.02.126>.
- [27] Koppenol, W.H., Stanbury, D.M., Bounds, P.L., 2010. Electrode potentials of partially reduced oxygen species, from dioxygen to water. *Free Radic Biol Med* 49, 317–322. <https://doi.org/10.1016/j.freeradbiomed.2010.04.011>.
- [28] Javed, H., Lyu, C., Sun, R., Zhang, D., Alvarez, P.J.J., 2020. Discerning the inefficiency of hydroxyl radicals during perfluorooctanoic acid degradation. *Chemosphere* 247. <https://doi.org/10.1016/j.chemosphere.2020.125883>.
- [29] Mitchell, S.M., Ahmad, M., Teel, A.L., Watts, R.J., 2013. Degradation of perfluorooctanoic acid by reactive species generated through catalyzed H₂O₂ propagation reactions. *Environ Sci Technol Lett* 1, 117–121. <https://doi.org/10.1021/ez4000862>.
- [30] Tang, H., Zhang, W., Meng, Y., Xia, S., 2021. A direct Z-scheme heterojunction with boosted transportation of photogenerated charge carriers for highly efficient photodegradation of PFOA: Reaction kinetics and mechanism. *Appl Catal B Environ* 285, 119851. <https://doi.org/10.1016/j.apcatb.2020.119851>.
- [31] Fu, S., Zhang, Y., Xu, X., Dai, X., Zhu, L., 2022. Peroxymonosulfate activation by iron self-doped sludge-derived biochar for degradation of perfluorooctanoic acid: A singlet oxygen-dominated nonradical pathway. *Chem Eng J* 450, 137953. <https://doi.org/10.1016/j.cej.2022.137953>.
- [32] Cheng, J., Fan, Y., Pei, X., Tian, D., Liu, Z., Wei, Z.Z., Ji, H.F., Chen, Q., 2022. Mechanism and reactive species in a fountain-strip DBD plasma for degrading perfluorooctanoic acid (PFOA). *Water* 14. <https://doi.org/10.3390/w14213384>.
- [33] Liu, G., Feng, C., Shao, P., 2021. Degradation of perfluorooctanoic acid with hydrated electron by a heterogeneous catalytic system. *Environ Sci Technol* 56, 6223–6231. <https://doi.org/10.1021/acs.est.1c06793>.
- [34] Wang, W., Chen, Y., Li, G., Gu, W., An, T., 2020. Photocatalytic reductive defluorination of perfluorooctanoic acid in water under visible light irradiation: The role of electron donor. *Environ Sci Water Res Technol* 6, 1638–1648. <https://doi.org/10.1039/d0ew00205d>.
- [35] Huang, D., Yin, L., Niu, J., 2016. Photoinduced hydrodefluorination mechanisms of perfluorooctanoic acid by the SiC/Graphene catalyst. *Environ Sci Technol* 50, 5857–5863. <https://doi.org/10.1021/acs.est.6b00652>.
- [36] Weon, S., Suh, M.-J., Chu, C., Huang, D., Stavitski, E., Kim, J.-H., 2021. Site-selective loading of single-atom Pt on TiO₂ for photocatalytic oxidation and reductive hydrodefluorination. *ACS EST Eng* 1, 512–522. <https://doi.org/10.1021/acsestengg.0c00210>.
- [37] Huang, D., De Vera, G.A., Chu, C., Zhu, Q., Stavitski, E., Mao, J., Xin, H., Spies, J. A., Schmuttenmaer, C.A., Niu, J., Haller, G.L., Kim, J.H., 2018. Single-atom Pt catalyst for effective C-F bond activation via hydrodefluorination. *ACS Catal* 8, 9353–9358. <https://doi.org/10.1021/acscatal.8b02660>.
- [38] Trojanowicz, M., Bojanowska-czajka, A., Bartosiewicz, I., Kulisa, K., 2018. Advanced Oxidation / Reduction Processes treatment for aqueous perfluorooctanoate (PFOA) and perfluorooctanesulfonate (PFOS) – A review of recent advances. *Chem Eng J* 336, 170–199. <https://doi.org/10.1016/j.cej.2017.10.153>.
- [39] Wei, Z., Xu, T., Zhao, D., 2019. Treatment of per- and polyfluoroalkyl substances in landfill leachate: Status, chemistry and prospects. *Environ Sci Water Res Technol* 5, 1814–1835. <https://doi.org/10.1039/c9ew00645a>.
- [40] Liang, X., Cheng, J., Yang, C., Yang, S., 2016. Factors influencing aqueous perfluorooctanoic acid (PFOA) photodecomposition by VUV irradiation in the presence of ferric ions. *Chem Eng J* 298, 291–299. <https://doi.org/10.1016/j.cej.2016.03.150>.
- [41] Cheng, J., Liang, X., Yang, S., Hu, Y., 2014. Photochemical defluorination of aqueous perfluorooctanoic acid (PFOA) by VUV/Fe³⁺ system. *Chem Eng J* 239, 242–249. <https://doi.org/10.1016/j.cej.2013.11.023>.
- [42] Li, X., Zhang, P., Jin, L., Shao, T., Li, Z., Cao, J., 2012. Efficient photocatalytic decomposition of perfluorooctanoic acid by indium oxide and its mechanism. *Environ Sci Technol* 46, 5528–5534. <https://doi.org/10.1021/es204279u>.
- [43] Chen, M.J., Lo, S.L., Lee, Y.C., Huang, C.C., 2015. Photocatalytic decomposition of perfluorooctanoic acid by transition-metal modified titanium dioxide. *J Hazard Mater* 288, 168–175. <https://doi.org/10.1016/j.jhazmat.2015.02.004>.
- [44] Chen, M.J., Lo, S.L., Lee, Y.C., Kuo, J., Wu, C.H., 2016. Decomposition of perfluorooctanoic acid by ultraviolet light irradiation with Pb-modified titanium dioxide. *J Hazard Mater* 303, 111–118. <https://doi.org/10.1016/j.jhazmat.2015.10.011>.
- [45] Estrellan, C.R., Salim, C., Hinode, H., 2010. Photocatalytic decomposition of perfluorooctanoic acid by iron and niobium co-doped titanium dioxide. *J Hazard Mater* 179, 79–83. <https://doi.org/10.1016/j.jhazmat.2010.02.060>.
- [46] Li, M., Yu, Z., Liu, Q., Sun, L., Huang, W., 2016. Photocatalytic decomposition of perfluorooctanoic acid by noble metallic nanoparticles modified TiO₂. *Chem Eng J* 286, 232–238. <https://doi.org/10.1016/j.cej.2015.10.037>.
- [47] Sansotera, M., Persico, F., Pirola, C., Navarrini, W., Di Michele, A., Bianchi, C.L., 2014. Decomposition of perfluorooctanoic acid photocatalyzed by titanium dioxide: Chemical modification of the catalyst surface induced by fluoride ions. *Appl Catal B Environ* 148–149, 29–35. <https://doi.org/10.1016/j.apcatb.2013.10.038>.
- [48] Gatto, S., Sansotera, M., Persico, F., Gola, M., Pirola, C., Panzeri, W., Navarrini, W., Bianchi, C.L., 2015. Surface fluorination on TiO₂ catalyst induced by photodegradation of perfluorooctanoic acid. *Catal Today* 241, 8–14. <https://doi.org/10.1016/j.cattod.2014.04.031>.
- [49] Chen, Y.C., Lo, S.L., Kuo, J., 2011. Effects of titanate nanotubes synthesized by a microwave hydrothermal method on photocatalytic decomposition of perfluorooctanoic acid. *Water Res* 45, 4131–4140. <https://doi.org/10.1016/j.watres.2011.05.020>.
- [50] Wu, Y., Li, Y., Tian, A., Mao, K., Liu, J., 2016. Selective removal of perfluorooctanoic acid using molecularly imprinted polymer-modified TiO₂ nanotube arrays. *Int J Photo* 2016, 1–10. <https://doi.org/10.1155/2016/7368795>.
- [51] Yao, X., Zuo, J., Wang, Y.J., Song, N.N., Li, H.H., Qiu, K., 2021. Enhanced photocatalytic degradation of perfluorooctanoic acid by mesoporous Sb₂O₃/TiO₂ heterojunctions. *Front Chem* 9, 1–10. <https://doi.org/10.3389/fchem.2021.690520>.
- [52] Arana Juve, J.M., Christensen, F.M.S., Wang, Y., Wei, Z., 2022. Electrodialysis for metal removal and recovery: A review. *Chem Eng J* 435, 134857. <https://doi.org/10.1016/j.cej.2022.134857>.
- [53] Samuel, M.S., Shang, M., Niu, J., 2022. Photocatalytic degradation of perfluoroalkyl substances in water by using a duo-functional tri-metallic-oxide hybrid catalyst. *Chemosphere* 293, 133568. <https://doi.org/10.1016/j.chemosphere.2022.133568>.
- [54] Awfa, D., Ateia, M., Fujii, M., Johnson, M.S., Yoshimura, C., 2018. Photodegradation of pharmaceuticals and personal care products in water treatment using carbonaceous-TiO₂ composites: A critical review of recent literature. *Water Res* 142, 26–45. <https://doi.org/10.1016/j.watres.2018.05.036>.
- [55] Song, C., Chen, P., Wang, C., Zhu, L., 2012. Photodegradation of perfluorooctanoic acid by synthesized TiO₂-MWCNT composites under 365nm UV irradiation. *Chemosphere* 86, 853–859. <https://doi.org/10.1016/j.chemosphere.2011.11.034>.
- [56] Li, F., Wei, Z., He, K., Blaney, L., Cheng, X., Xu, T., Liu, W., Zhao, D., 2020. A concentrate-and-destroy technique for degradation of perfluorooctanoic acid in water using a new adsorptive photocatalyst. *Water Res* 185, 1–14. <https://doi.org/10.1016/j.watres.2020.116219>.
- [57] Arana Juve, J.-M., Li, F., Zhu, Y., Liu, W., Ottosen, L.D.M., Zhao, D., Wei, Z., 2022. Concentrate and degrade PFOA with a photo-regenerable composite of In-doped TNTs@AC. *Chemosphere* 300, 134495. <https://doi.org/10.1016/j.chemosphere.2022.134495>.
- [58] Zhu, Y., Xu, T., Zhao, D., Li, F., Liu, W., Wang, B., An, B., 2021. Adsorption and solid-phase photocatalytic degradation of perfluorooctane sulfonate in water using gallium-doped carbon-modified titanate nanotubes. *Chem Eng J* 421, 129676. <https://doi.org/10.1016/j.cej.2021.129676>.
- [59] Tian, S., Xu, T., Fang, L., Zhu, Y., Li, F., Leary, R.N., Zhang, M., Zhao, D., Soong, T.Y., Shi, H., 2021. A ‘Concentrate-&-Destroy’ technology for enhanced removal and destruction of per- and polyfluoroalkyl substances in municipal landfill leachate. *Sci Total Environ* 791, 148124. <https://doi.org/10.1016/j.scitotenv.2021.148124>.
- [60] Zhu, Y., Ji, H., He, K., Blaney, L., Xu, T., Zhao, D., 2022. Photocatalytic degradation of GenX in water using a new adsorptive photocatalyst. *Water Res* 220. <https://doi.org/10.1016/j.watres.2022.118650>.
- [61] Park, K., Ali, I., Kim, J.O., 2018. Photodegradation of perfluorooctanoic acid by graphene oxide-deposited TiO₂ nanotube arrays in aqueous phase. *J Environ Manag* 218, 333–339. <https://doi.org/10.1016/j.jenvman.2018.04.016>.
- [62] Panchangam, S.C., Yellatur, C.S., Yang, J.S., Loka, S.S., Lin, A.Y.C., Vemula, V., 2018. Facile fabrication of TiO₂-graphene nanocomposites (TGNCs) for the efficient photocatalytic oxidation of perfluorooctanoic acid (PFOA). *J Environ Chem Eng* 6, 6359–6369. <https://doi.org/10.1016/j.jece.2018.10.003>.
- [63] Konkna, B., Vasudevan, S., 2012. Understanding aqueous dispersibility of graphene oxide and reduced graphene oxide through pKa measurements. *J Phys Chem Lett* 3, 867–872. <https://doi.org/10.1021/jz300236w>.
- [64] Zhu, C., Xu, J., Song, S., Wang, J., Li, Y., Liu, R., Shen, Y., 2020. TiO₂ quantum dots loaded sulfonated graphene aerogel for effective adsorption-photocatalysis of PFOA. *Sci Total Environ* 698, 134275. <https://doi.org/10.1016/j.scitotenv.2019.134275>.
- [65] Jiang, X., Wang, W., Yu, G., Deng, S., 2021. Contribution of Nanobubbles for PFAS Adsorption on Graphene and OH- And NH₂-Functionalized Graphene: Comparing Simulations with Experimental Results. *Environ Sci Technol* 55, 13254–13263. <https://doi.org/10.1021/acs.est.1c03022>.
- [66] Kong, Z., Lu, L., Zhu, C., Xu, J., Fang, Q., Liu, R., Shen, Y., 2022. Enhanced adsorption and photocatalytic removal of PFOA from water by F-functionalized

- MOF with in-situ-growth TiO₂: Regulation of electron density and bandgap. *Sep Purif Technol* 297, 121449. <https://doi.org/10.1016/j.seppur.2022.121449>.
- [67] Bouteh, E., Bentel, M.J., Cates, E.L., 2023. Semiconductor-hydrophobic material interfaces as a new active site paradigm for photocatalytic degradation of perfluorocarboxylic acids. *J Hazard Mater* 453, 131437. <https://doi.org/10.1016/j.jhazmat.2023.131437>.
- [68] Wang, Y., Zhang, P., Pan, G., Chen, H., 2008. Ferric ion mediated photochemical decomposition of perfluorooctanoic acid (PFOA) by 254 nm UV light. *J Hazard Mater* 160, 181–186. <https://doi.org/10.1016/j.jhazmat.2008.02.105>.
- [69] Chen, Y., Ma, H., Zhu, J., Gu, Y., Liu, T., 2022. New insights into ferric iron-facilitated UV254 photolytic defluorination of perfluorooctanoic acid (PFOA): Combined experimental and theoretical study. *J Hazard Mater* 434, 128865. <https://doi.org/10.1016/j.jhazmat.2022.128865>.
- [70] Liu, D., Xiu, Z., Liu, F., Wu, G., Adamson, D., Newell, C., Vikesland, P., Tsai, A.L., Alvarez, P.J., 2013. Perfluorooctanoic acid degradation in the presence of Fe(III) under natural sunlight. *J Hazard Mater* 262, 456–463. <https://doi.org/10.1016/j.jhazmat.2013.09.001>.
- [71] Ohno, M., Ito, M., Ohkura, R., Mino A, E.R., Kose, T., Okuda, T., Nakai, S., Kawata, K., Nishijima, W., 2014. Photochemical decomposition of perfluorooctanoic acid mediated by iron in strongly acidic conditions. *J Hazard Mater* 268, 150–155. <https://doi.org/10.1016/j.jhazmat.2013.12.059>.
- [72] Xia, C., Liu, J., 2020. Degradation of perfluorooctanoic acid by zero-valent iron nanoparticles under ultraviolet light. *J Nanopart Res* 22, 188. <https://doi.org/10.1007/s11051-020-04925-4>.
- [73] Qian, L., Georgi, A., Gonzalez-Olmos, R., Kopinke, F.D., 2020. Degradation of perfluorooctanoic acid adsorbed on Fe-zeolites with molecular oxygen as oxidant under UV-A irradiation. *Appl Catal B Environ* 278, 119283. <https://doi.org/10.1016/j.apcatb.2020.119283>.
- [74] Xu, T., Ji, H., Gu, Y., Tong, T., Xia, Y., Zhang, L., Zhao, D., 2020. Enhanced adsorption and photocatalytic degradation of perfluorooctanoic acid in water using iron (hydr)oxides/carbon sphere composite. *Chem Eng J* 388, 124230. <https://doi.org/10.1016/j.cej.2020.124230>.
- [75] Edwards, D.F., 1997. Beta-Gallium Oxide (β -Ga₂O₃). *Handb Opt Constants Solids* 3, 753–760.
- [76] Zhao, B., Lv, M., Zhou, L., 2012. Photocatalytic degradation of perfluorooctanoic acid with β -Ga₂O₃ in anoxic aqueous solution. *J Environ Sci* 24, 774–780. [https://doi.org/10.1016/S1001-0742\(11\)60818-8](https://doi.org/10.1016/S1001-0742(11)60818-8).
- [77] Zhao, B., Zhang, P., 2009. Photocatalytic decomposition of perfluorooctanoic acid with β -Ga₂O₃ wide bandgap photocatalyst. *Catal Commun* 10, 1184–1187. <https://doi.org/10.1016/j.catcom.2009.01.017>.
- [78] Shao, T., Zhang, P., Li, Z., Jin, L., 2013. Photocatalytic decomposition of perfluorooctanoic acid in pure water and wastewater by needle-like nanostructured gallium oxide. *Chin J Catal* 34, 1551–1559. [https://doi.org/10.1016/S1872-2067\(12\)60612-3](https://doi.org/10.1016/S1872-2067(12)60612-3).
- [79] Tan, X., Chen, G., Xing, D., Ding, W., Liu, H., Li, T., Huang, Y., 2020. Indium-modified Ga₂O₃ hierarchical nanosheets as efficient photocatalysts for the degradation of perfluorooctanoic acid. *Environ Sci Nano* 7, 2229–2239. <https://doi.org/10.1039/d0en00259c>.
- [80] Shao, T., Zhang, P., Jin, L., Li, Z., 2013. Photocatalytic decomposition of perfluorooctanoic acid in pure water and sewage water by nanostructured gallium oxide. *Appl Catal B Environ* 142–143, 654–661. <https://doi.org/10.1016/j.apcatb.2013.05.074>.
- [81] Zhao, B., Li, X., Yang, L., Wang, F., Li, J., Xia, W., Li, W., Zhou, L., Zhao, C., 2015. β -Ga₂O₃ nanorod synthesis with a one-step microwave irradiation hydrothermal method and its efficient photocatalytic degradation for perfluorooctanoic acid. *Photochem Photobiol* 91, 42–47. <https://doi.org/10.1111/php.12383>.
- [82] Xu, J., Wu, M., Yang, J., Wang, Z., Chen, M., Teng, F., 2017. Efficient photocatalytic degradation of perfluorooctanoic acid by a wide band gap p-block metal oxyhydroxide InOOH. *Appl Surf Sci* 416, 587–592. <https://doi.org/10.1016/j.apsusc.2017.04.040>.
- [83] Li, Z., Zhang, P., Shao, T., Li, X., 2012. In₂O₃ nanoporous nanosphere: A highly efficient photocatalyst for decomposition of perfluorooctanoic acid. *Appl Catal B Environ* 125, 350–357. <https://doi.org/10.1016/j.apcatb.2012.06.017>.
- [84] Li, Z., Zhang, P., Shao, T., Wang, J., Jin, L., Li, X., 2013. Different nanostructured In₂O₃ for photocatalytic decomposition of perfluorooctanoic acid (PFOA). *J Hazard Mater* 260, 40–46. <https://doi.org/10.1016/j.jhazmat.2013.04.042>.
- [85] Li, Z., Zhang, P., Li, J., Shao, T., Wang, J., Jin, L., 2014. Synthesis of In₂O₃ porous nanoplates for photocatalytic decomposition of perfluorooctanoic acid (PFOA). *Catal Commun* 43, 42–46. <https://doi.org/10.1016/j.catcom.2013.09.004>.
- [86] Xu, C., Qiu, P., Chen, H., Jiang, F., Wang, X., 2019. Fabrication of two-dimensional indium oxide nanosheets with graphitic carbon nitride nanosheets as sacrificial templates. *Mater Lett* 242, 24–27. <https://doi.org/10.1016/j.matlet.2019.01.101>.
- [87] Nekouei, F., Wen, X., Zheng, Z., Sun, Q., Lu, T., Orton, H., Kremer, F., Nekouei, S., Yuan, T., Abdelkader, E.H., Liu, B., Tricoli, A., Otting, G., Liu, Z., Frankcombe, T., Liu, Y., 2022. InOOH-mediated intergrown heterojunctions for enhanced photocatalytic Performance: Assembly and interfacial charge carrier transferring. *Chem Eng J* 442, 136355. <https://doi.org/10.1016/j.cej.2022.136355>.
- [88] Liu, X., Xu, B., Duan, X., Hao, Q., Wei, W., Wang, S., Ni, B.J., 2021. Facile preparation of hydrophilic In₂O₃ nanospheres and rods with improved performances for photocatalytic degradation of PFOA. *Environ Sci Nano* 8, 1010–1018. <https://doi.org/10.1039/d0en01216e>.
- [89] Liu, J., Guo, C., Wu, N., Li, C., Qu, R., Wang, Z., Jin, R., Qiao, Y., He, Z., Lu, J., Feng, X., Zhang, Y., Wang, A., 2022. Efficient photocatalytic degradation of PFOA in N-doped In₂O₃ / simulated sunlight irradiation system and its mechanism. *Chem Eng J* 435, 134627. <https://doi.org/10.1016/j.cej.2022.134627>.
- [90] Liu, X., Chen, Z., Tian, K., Zhu, F., Hao, D., Cheng, D., Wei, W., Zhang, L., Ni, B., 2021. Fe³⁺ promoted the photocatalytic defluorination of perfluorooctanoic acid (PFOA) over In₂O₃. *ACS EST Water* 1, 2431–2439. <https://doi.org/10.1021/acestwater.1c00275>.
- [91] Li, Z., Zhang, P., Li, J., Shao, T., Jin, L., 2013. Synthesis of In₂O₃-graphene composites and their photocatalytic performance towards perfluorooctanoic acid decomposition. *J Photochem Photobiol A Chem* 271, 111–116. <https://doi.org/10.1016/j.jphotochem.2013.08.012>.
- [92] Wu, Y., Li, Y., Fang, C., Li, C., 2019. Highly efficient degradation of perfluorooctanoic acid over a MnOx-modified oxygen-vacancy-rich In₂O₃ photocatalyst. *ChemCatChem* 11, 2297–2303. <https://doi.org/10.1002/cctc.201900273>.
- [93] Jiang, F., Zhao, H., Chen, H., Xu, C., Chen, J., 2016. Enhancement of photocatalytic decomposition of perfluorooctanoic acid on CeO₂/In₂O₃. *RSC Adv* 6, 72015–72021. <https://doi.org/10.1039/c6ra09856h>.
- [94] Xu, C., Qiu, P., Chen, H., Jiang, F., 2017. Platinum modified indium oxide nanorods with enhanced photocatalytic activity on degradation of perfluorooctanoic acid (PFOA). *J Taiwan Inst Chem Eng* 80, 761–768. <https://doi.org/10.1016/j.jtice.2017.09.018>.
- [95] Wang, J., Cao, C., Zhang, Y., Zhang, Y., Zhu, L., 2021. Underneath mechanisms into the super effective degradation of PFOA by BiOF nanosheets with tunable oxygen vacancies on exposed (101) facets. *Appl Catal B Environ* 286, 119911. <https://doi.org/10.1016/j.apcatb.2021.119911>.
- [96] Zhang, K.L., Liu, C.M., Huang, F.Q., Zheng, C., Wang, W.D., 2006. Study of the electronic structure and photocatalytic activity of the BiOCl photocatalyst. *Appl Catal B Environ* 68, 125–129. <https://doi.org/10.1016/j.apcatb.2006.08.002>.
- [97] Zhao, L., Zhang, X., Fan, C., Liang, Z., Han, P., 2012. First-principles study on the structural, electronic and optical properties of BiOX (X=Cl, Br, I) crystals. *Phys B Condens Matter* 407, 3364–3370. <https://doi.org/10.1016/j.physb.2012.04.039>.
- [98] Jiang, J., Zhao, K., Xiao, X., Zhang, L., 2012. Synthesis and facet-dependent photoreactivity of BiOCl single-crystalline nanosheets. *J Am Chem Soc* 134, 4473–4476. <https://doi.org/10.1021/ja210484t>.
- [99] Wang, J., Cao, C., Wang, J., Zhang, Y., Zhu, L., 2022. Insights into highly efficient photodegradation of poly/perfluoroalkyl substances by In-MOF/BiOF heterojunctions: Built-in electric field and strong surface adsorption. *Appl Catal B Environ* 304, 121013. <https://doi.org/10.1016/j.apcatb.2021.121013>.
- [100] Zhong, J., Zhao, Y., Ding, L., Ji, H., Ma, W., Chen, C., Zhao, J., 2019. Opposite photocatalytic oxidation behaviors of BiOCl and TiO₂: Direct hole transfer vs. indirect •OH oxidation. *Appl Catal B Environ* 241, 514–520. <https://doi.org/10.1016/j.apcatb.2018.09.058>.
- [101] Dong, X.D., Zhang, Y.M., Zhao, Z.Y., 2021. Role of the polar electric field in bismuth oxyhalides for photocatalytic water splitting. *Inorg Chem* 60, 8461–8474. <https://doi.org/10.1021/acs.inorgchem.0c03220>.
- [102] Wu, Y., Hu, Y., Han, M., Ouyang, Y., Xia, L., Huang, X., Hu, Z., Li, C., 2021. Mechanism insights into the facet-dependent photocatalytic degradation of perfluorooctanoic acid on BiOCl nanosheets. *Chem Eng J* 425, 130672. <https://doi.org/10.1016/j.cej.2021.130672>.
- [103] Liao, H., Zhong, J., Li, J., 2022. Tunable oxygen vacancies facilitated removal of PFOA and RhB over BiOCl prepared with alcohol ether sulphate. *Appl Surf Sci* 590, 152891. <https://doi.org/10.1016/j.apsusc.2022.152891>.
- [104] Sun, Y., Li, G., Wang, W., Gu, W., Wong, P.K., An, T., 2019. Photocatalytic defluorination of perfluorooctanoic acid by surface defective BiOCl: Fast microwave solvothermal synthesis and photocatalytic mechanisms. *J Environ Sci (China)* 84, 69–79. <https://doi.org/10.1016/j.jes.2019.04.012>.
- [105] Liu, H., Huang, J., Chen, J., Zhong, J., Li, J., Ma, D., 2020. Influence of different solvents on the preparation and photocatalytic property of BiOCl toward decontamination of phenol and perfluorooctanoic acid. *Chem Phys Lett* 748. <https://doi.org/10.1016/j.cplett.2020.137401>.
- [106] Song, Z., Dong, X., Fang, J., Xiong, C., Wang, N., Tang, X., 2019. Improved photocatalytic degradation of perfluorooctanoic acid on oxygen vacancies-tunable bismuth oxychloride nanosheets prepared by a facile hydrolysis. *J Hazard Mater* 377, 371–380. <https://doi.org/10.1016/j.jhazmat.2019.05.084>.
- [107] Yang, C., He, Y., Zhong, J., Li, J., 2022. Photocatalytic performance of rich Ov-BiOCl modified by polyphenylene sulfide. *Adv Powder Technol* 33, 103427. <https://doi.org/10.1016/j.apt.2022.103427>.
- [108] Wang, J., Cao, C., Wang, Y., Wang, Y., Sun, B., Zhu, L., 2020. In situ preparation of p-n BiOI@Bi₅O₇I heterojunction for enhanced PFOA photocatalytic degradation under simulated solar light irradiation. *Chem Eng J* 391, 123530. <https://doi.org/10.1016/j.cej.2019.123530>.
- [109] Yang, Y., Ji, W., Li, X., Zheng, Z., Bi, F., Yang, M., Xu, J., Zhang, X., 2021. Insights into the degradation mechanism of perfluorooctanoic acid under visible-light irradiation through fabricating flower-shaped Bi₅O₇I/ZnO n-n heterojunction microspheres. *Chem Eng J* 420, 129934. <https://doi.org/10.1016/j.cej.2021.129934>.
- [110] Wang, J., Wang, Y., Cao, C., Zhang, Y., Zhang, Y., Zhu, L., 2021. Decomposition of highly persistent perfluorooctanoic acid by hollow Bi/BiOI_{1-x}F_x: Synergistic effects of surface plasmon resonance and modified band structures. *J Hazard Mater* 402, 123459. <https://doi.org/10.1016/j.jhazmat.2020.123459>.
- [111] Li, T., Wang, C., Wang, T., Zhu, L., 2020. Highly efficient photocatalytic degradation toward perfluorooctanoic acid by bromine doped BiOI with high exposure of (001) facet. *Appl Catal B Environ* 268, 118442. <https://doi.org/10.1016/j.apcatb.2019.118442>.
- [112] Low, J., Yu, J., Jaroniec, M., Wageh, S., Al-Ghamdi, A.A., 2017. Heterojunction photocatalysts. *Adv Mater* 29, 1601694. <https://doi.org/10.1002/adma.201601694>.

- [113] Liu, X., Duan, X., Bao, T., Hao, D., Chen, Z., Wei, W., Wang, D., Wang, S., Ni, B., 2022. High-performance photocatalytic decomposition of PFOA by BiOX/TiO₂ heterojunctions: Self-induced inner electric fields and band alignment. *J Hazard Mater* 430, 128195. <https://doi.org/10.1016/j.jhazmat.2021.128195>.
- [114] Chen, F., He, A., Wang, Y., Yu, W., Chen, H., Geng, F., Li, Z., Zhou, Z., Liang, Y., Fu, J., Zhao, L., Wang, Y., 2022. Efficient photodegradation of PFOA using spherical BiOBr modified TiO₂ via hole-remained oxidation mechanism. *Chemosphere* 298, 134176. <https://doi.org/10.1016/j.chemosphere.2022.134176>.
- [115] Qanbarzadeh, M., Wang, D., Ateia, M., Sahu, S.P., Cates, E.L., 2021. Impacts of reactor configuration, degradation mechanisms, and water matrices on perfluorocarboxylic acid treatment efficiency by the UV/Bi₃O(OH)(PO₄)₂ photocatalytic process. *ACS EST Eng* 1, 239–248. <https://doi.org/10.1021/acsestengg.0c00086>.
- [116] Sahu, S.P., Qanbarzadeh, M., Ateia, M., Torzkadeh, H., Maroli, A.S., Cates, E.L., 2018. Rapid degradation and mineralization of perfluorooctanoic acid by a new petitjeanite Bi₃O(OH)(PO₄)₂ microparticle ultraviolet photocatalyst. *Environ Sci Technol Lett* 5, 533–538. <https://doi.org/10.1021/acs.estlett.8b00395>.
- [117] Bacha, A.U.R., Nabi, I., Fu, Z., Li, K., Cheng, H., Zhang, L., 2019. A comparative study of bismuth-based photocatalysts with titanium dioxide for perfluorooctanoic acid degradation. *Chin Chem Lett* 30, 2225–2230. <https://doi.org/10.1016/j.ccl.2019.07.058>.
- [118] Tan, X., Jiang, Z., Huang, Y., 2023. Photo-induced surface frustrated Lewis pairs for promoted photocatalytic decomposition of perfluorooctanoic acid. *Front Environ Sci Eng* 17 (1), 6. <https://doi.org/10.1007/s11783-023-1603-6>.
- [119] Bentel, M.J., Mason, M.M., Cates, E.L., 2023. Synthesis of Petitjeanite Bi₃O(OH)(PO₄)₂ Photocatalytic Microparticles: Effect of Synthetic Conditions on the Crystal Structure and Activity toward Degradation of Aqueous Perfluorooctanoic Acid (PFOA). *ACS Appl Mater Interfaces* 4. <https://doi.org/10.1021/acami.2c20483>.
- [120] Gu, M., Li, S., Fan, X., Huang, J., Yu, G., 2022. Effective breaking of the fluorocarbon chain by the interface Bi₂O₂X--PFOA complex strategy via coordinated Se on construction of the internal photogenerated carrier pathway. *ACS Appl Mater Interfaces* 14, 654–667. <https://doi.org/10.1021/acami.1c17406>.
- [121] Noori, F., Gholizadeh, A., 2019. Structural, optical, magnetic properties and visible light photocatalytic activity of BiFeO₃/graphene oxide nanocomposites. *Mater Res Express* 6, 0–13. <https://doi.org/10.1088/2053-1591/ab6807>.
- [122] Shang, E., Li, Y., Niu, J., Li, S., Zhang, G., Wang, X., 2018. Photocatalytic degradation of perfluorooctanoic acid over Pb-BiFeO₃/rGO catalyst: Kinetics and mechanism. *Chemosphere* 211, 34–43. <https://doi.org/10.1016/j.chemosphere.2018.07.130>.
- [123] Xu, T., Zhu, Y., Duan, J., Xia, Y., Tong, T., Zhang, L., Zhao, D., 2020. Enhanced photocatalytic degradation of perfluorooctanoic acid using carbon-modified bismuth phosphate composite: Effectiveness, material synergy and roles of carbon. *Chem Eng J* 395, 124991. <https://doi.org/10.1016/j.cej.2020.124991>.
- [124] You, X., Yu, L., Xiao, F., Wu, S., Yang, C., Cheng, J., 2018. Synthesis of phosphotungstic acid-supported bimodal mesoporous silica-based catalyst for defluorination of aqueous perfluorooctanoic acid under vacuum UV irradiation. *Chem Eng J* 335, 812–821. <https://doi.org/10.1016/j.cej.2017.10.123>.
- [125] Duan, L., Wang, B., Heck, K., Guo, S., Clark, C.A., Arredondo, J., Wang, M., Senftle, T.P., Westerhoff, P., Wen, X., Song, Y., Wong, M.S., 2020. Efficient photocatalytic PFOA degradation over boron nitride. *Environ Sci Technol Lett* 7, 613–619. <https://doi.org/10.1021/acs.estlett.0c00434>.
- [126] Duan, L., Wang, B., Heck, K.N., Clark, C.A., Wei, J., Wang, M., Metz, J., Wu, G., Tsai, A.L., Guo, S., Arredondo, J., Mohite, A.D., Senftle, T.P., Westerhoff, P., Alvarez, P., Wen, X., Song, Y., Wong, M.S., 2022. Titanium oxide improves boron nitride photocatalytic degradation of perfluorooctanoic acid. *Chem Eng J* 448, 137735. <https://doi.org/10.1016/j.cej.2022.137735>.
- [127] Song, H., Wang, Y., Ling, Z., Zu, D., Li, Z., Shen, Y., Li, C., 2020. Enhanced photocatalytic degradation of perfluorooctanoic acid by Ti₃C₂ MXene-derived heterojunction photocatalyst: Application of intercalation strategy in DESs. *Sci Total Environ* 746, 141009. <https://doi.org/10.1016/j.scitotenv.2020.141009>.
- [128] Bhat, A., Anwer, S., Bhat, K.S., Mohideen, M.I.H., Liao, K., Qurashi, A., 2021. Prospects challenges and stability of 2D MXenes for clean energy conversion and storage applications. *2D Mater Appl* 5, 1–21. <https://doi.org/10.1038/s41699-021-00239-8>.
- [129] Li, S., Zhang, G., Zhang, W., Zheng, H., Zhu, W., Sun, N., Zheng, Y., Wang, P., 2017. Microwave enhanced Fenton-like process for degradation of perfluorooctanoic acid (PFOA) using Pb-BiFeO₃/rGO as heterogeneous catalyst. *Chem Eng J* 326, 756–764. <https://doi.org/10.1016/j.cej.2017.06.037>.
- [130] Zhang, Y., Sun, A., Xiong, M., Macharia, D.K., Liu, J., Chen, Z., Li, M., Zhang, L., 2021. TiO₂/BiOI p-n junction-decorated carbon fibers as weavable photocatalyst with UV-vis photoresponsive for efficiently degrading various pollutants. *Chem Eng J* 415, 129019. <https://doi.org/10.1016/j.cej.2021.129019>.
- [131] Rivero, M.J., Ribao, P., Gomez-Ruiz, B., Urriaga, A., Ortiz, I., 2020. Comparative performance of TiO₂-rGO photocatalyst in the degradation of dichloroacetic and perfluorooctanoic acids. *Sep Purif Technol* 240, 116637. <https://doi.org/10.1016/j.seppur.2020.116637>.
- [132] Shen, H.L., Hu, H.H., Liang, D.Y., Meng, H.L., Li, P.G., Tang, W.H., Cui, C., 2012. Effect of calcination temperature on the microstructure, crystallinity and photocatalytic activity of TiO₂ hollow spheres. *J Alloy Compd* 542, 32–36. <https://doi.org/10.1016/j.jallcom.2012.07.080>.
- [133] Zak, A.K., Abrishami, M.E., Majid, W.H.A., Yousefi, R., Hosseini, S.M., 2011. Effects of annealing temperature on some structural and optical properties of ZnO nanoparticles prepared by a modified sol-gel combustion method. *Ceram Int* 37, 393–398. <https://doi.org/10.1016/j.ceramint.2010.08.017>.
- [134] Anjum, S., Tufail, R., Rashid, K., Zia, R., Riaz, S., 2017. Effect of cobalt doping on crystallinity, stability, magnetic and optical properties of magnetic iron oxide nano-particles. *J Magn Magn Mater* 432, 198–207. <https://doi.org/10.1016/j.jmmm.2017.02.006>.
- [135] Gallagher, R.P., Lee, T.K., 2006. Adverse effects of ultraviolet radiation: A brief review. *Prog Biophys Mol Biol* 92, 119–131. <https://doi.org/10.1016/j.pbiomolbio.2006.02.011>.
- [136] Braham, R.J., Harris, A.T., 2009. Review of major design and scale-up considerations for solar photocatalytic reactors. *Ind Eng Chem Res* 48, 8890–8905. <https://doi.org/10.1021/ie900859z>.
- [137] Marcelino, R.B.P., Amorim, C.C., 2019. Towards visible-light photocatalysis for environmental applications: band-gap engineering versus photons absorption — a review. *Environ Sci Pollut Res* 26, 4155–4170. <https://doi.org/10.1007/s11356-018-3117-5>.
- [138] Sun, Q., Zhao, C., Frankcombe, T.J., Liu, H., Liu, Y., 2020. Heterogeneous photocatalytic decomposition of per- and poly-fluoroalkyl substances: A review. *Crit Rev Environ Sci Technol* 50, 523–547. <https://doi.org/10.1080/10643389.2019.1631988>.
- [139] Martín-Sómer, M., Pablos, C., van Grieken, R., Marugán, J., 2017. Influence of light distribution on the performance of photocatalytic reactors: LED vs mercury lamps. *Appl Catal B Environ* 215, 1–7. <https://doi.org/10.1016/j.apcatb.2017.05.048>.
- [140] Carbonaro, S., Sugihara, M.N., Strathmann, T.J., 2013. Continuous-flow photocatalytic treatment of pharmaceutical micropollutants: Activity, inhibition, and deactivation of TiO₂ photocatalysts in wastewater effluent. *Appl Catal B Environ* 129, 1–12. <https://doi.org/10.1016/j.apcatb.2012.09.014>.
- [141] Silva, D.B., Buttiglieri, G., Babi, S., 2021. State-of-the-art and current challenges for TiO₂/UV-LED photocatalytic degradation of emerging organic micropollutants. *Environ Sci Pollut Res* 28, 103–120. <https://doi.org/10.1007/s11356-020-11125-z>.
- [142] Gomez-Ruiz, B., Ribao, P., Diban, N., Rivero, M.J., Ortiz, I., Urriaga, A., 2018. Photocatalytic degradation and mineralization of perfluorooctanoic acid (PFOA) using a composite TiO₂-rGO catalyst. *J Hazard Mater* 344, 950–957. <https://doi.org/10.1016/j.jhazmat.2017.11.048>.
- [143] Lath, S., Knight, E.R., Navarro, D.A., Kookana, R.S., McLaughlin, M.J., 2019. Sorption of PFOA onto different laboratory materials: Filter membranes and centrifuge tubes. *Chemosphere* 222, 671–678. <https://doi.org/10.1016/j.chemosphere.2019.01.096>.
- [144] Zhang, D., Lee, C., Javed, H., Yu, P., Kim, J.H., Alvarez, P.J.J., 2018. Easily recoverable, micrometer-sized TiO₂ hierarchical spheres decorated with cyclodextrin for enhanced photocatalytic degradation of organic micropollutants. *Environ Sci Technol* 52, 12402–12411. <https://doi.org/10.1021/acs.est.8b04301>.
- [145] Liu, C.J., Murray, C.C., Marshall, R.E., Strathmann, T.J., Bellona, C., 2022. Removal of per- and polyfluoroalkyl substances from contaminated groundwater by granular activated carbon and anion exchange resins: a pilot-scale comparative assessment. *Environ Sci Water Res Technol* 8, 2245–2253. <https://doi.org/10.1039/d2ew00080f>.
- [146] Rani, C.N., Karthikeyan, S., Prince Arockia Doss, S., 2021. Photocatalytic ultrafiltration membrane reactors in water and wastewater treatment - A review. *Chem Eng Process - Process Intensif* 165, 108445. <https://doi.org/10.1016/j.cep.2021.108445>.
- [147] Van der Bruggen, B., Mänttäri, M., Nyström, M., 2008. Drawbacks of applying nanofiltration and how to avoid them: A review. *Sep Purif Technol* 63, 251–263. <https://doi.org/10.1016/j.seppur.2008.05.010>.
- [148] Iervolino, G., Zammit, I., Vaiano, V., Rizzo, L., 2020. Limitations and prospects for wastewater treatment by UV and visible-light-active heterogeneous photocatalysis: A critical review. In: Muñoz-Batista, M.J., Muñoz, A.N., Luque, R. (Eds.), *Top. Curr. Chem.* Springer, Cham, Switzerland, pp. 225–264. <https://doi.org/10.1007/s41061-019-0272-1>.
- [149] fang Li, M., guo Liu, Y., ming Zeng, G., Liu, N., bo Liu, S., 2019. Graphene and graphene-based nanocomposites used for antibiotics removal in water treatment: A review. *Chemosphere* 226, 360–380. <https://doi.org/10.1016/j.chemosphere.2019.03.117>.
- [150] Yang, Y., Zheng, Z., Ji, W., Xu, J., Zhang, X., 2020. Insights to perfluorooctanoic acid adsorption micro-mechanism over Fe-based metal organic frameworks: Combining computational calculation with response surface methodology. *J Hazard Mater* 395, 122686. <https://doi.org/10.1016/j.jhazmat.2020.122686>.
- [151] Yang, L., Xu, L., Bai, X., Jin, P., 2019. Enhanced visible-light activation of persulfate by Ti³⁺ self-doped TiO₂/graphene nanocomposite for the rapid and efficient degradation of micropollutants in water. *J Hazard Mater* 365, 107–117. <https://doi.org/10.1016/j.jhazmat.2018.10.090>.
- [152] Tian, D., Geng, D., Tyler Mehler, W., Goss, G., Wang, T., Yang, S., Niu, Y., Zheng, Y., Zhang, Y., 2021. Removal of perfluorooctanoic acid (PFOA) from aqueous solution by amino-functionalized graphene oxide (AGO) aerogels: Influencing factors, kinetics, isotherms, and thermodynamic studies. *Sci Total Environ* 783, 147041. <https://doi.org/10.1016/j.scitotenv.2021.147041>.
- [153] Liu, W., Cai, Z., Zhao, X., Wang, T., Li, F., Zhao, D., 2016. High-capacity and photoregenerable composite material for efficient adsorption and degradation of phenanthrene in water. *Environ Sci Technol* 50, 11174–11183. <https://doi.org/10.1021/acs.est.6b02623>.
- [154] Tian, S., Xu, T., Fang, L., Zhu, Y., Li, F., Leary, R.N., Zhang, M., Zhao, D., Soong, T. Y., Shi, H., 2021. A 'Concentrate-&Destroy' technology for enhanced removal and destruction of per- and polyfluoroalkyl substances in municipal landfill

- leachate. *Sci Total Environ* 791, 148124. <https://doi.org/10.1016/j.scitotenv.2021.148124>.
- [155] Plakas, K.V., Sarasidis, V.C., Patsios, S.I., Lambropoulou, D.A., Karabelas, A.J., 2016. Novel pilot scale continuous photocatalytic membrane reactor for removal of organic micropollutants from water. *Chem Eng J* 304, 335–343. <https://doi.org/10.1016/j.cej.2016.06.075>.
- [156] Zaib, Q., Mansoor, B., Ahmad, F., 2013. Photo-regenerable multi-walled carbon nanotube membranes for the removal of pharmaceutical micropollutants from water. *Environ Sci Process Impacts* 15, 1582–1589. <https://doi.org/10.1039/c3em00150d>.
- [157] Petala, A., Spyrou, D., Frontistis, Z., Mantzavinos, D., Kondarides, D.I., 2019. Immobilized Ag₃PO₄ photocatalyst for micro-pollutants removal in a continuous flow annular photoreactor. *Catal Today* 328, 223–229. <https://doi.org/10.1016/j.cattod.2018.10.062>.
- [158] Alvey, J., Dev, S., Quiñones, O., Dickenson, E., Aggarwal, S., Dotson, A., 2023. Photocatalytic membrane reactor utilizing immobile photocatalytic active layer on membranes for the removal of micropollutants. *ACS EST Water* 3, 1050–1059. <https://doi.org/10.1021/acsestwater.2c00528>.